Cell Reports
Medicine

Article

Selective and replicable neuroimaging-based indicators of pain discriminability

Graphical abstract

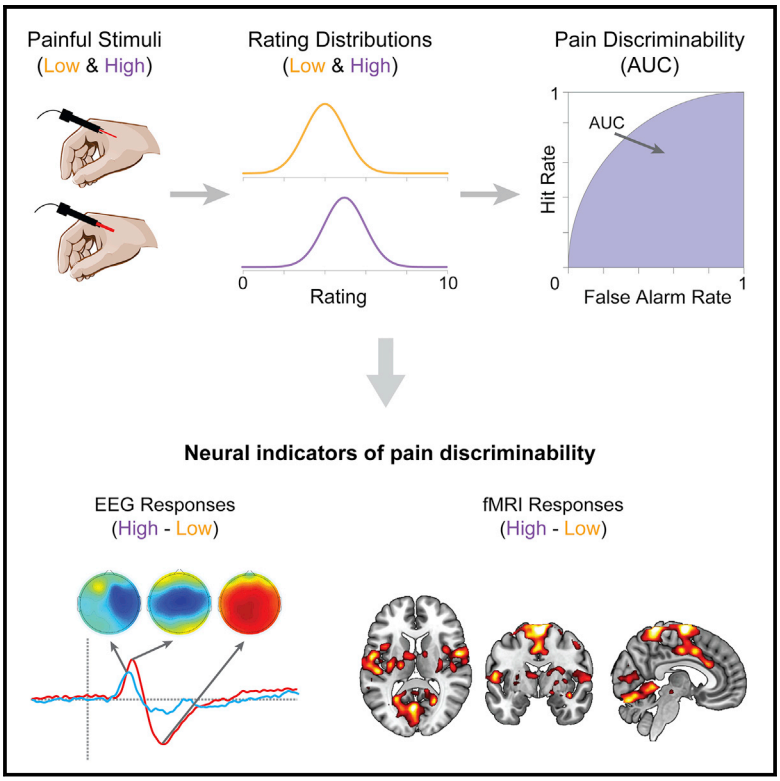

Highlights

- Discriminability is quantified by measures derived from signal detection theory
- Pain-evoked brain responses reliably correlate with pain discriminability
- The neural indicators of pain discriminability are pain selective
- Our findings are replicated in independent datasets sampled by different techniques

Authors

Li-Bo Zhang, Xue-Jing Lu, Gan Huang, Hui-Juan Zhang, Yi-Heng Tu, Ya-Zhuo Kong, Li Hu

Correspondence

huli@psych.ac.cn

In brief

The ability to discriminate between painful stimuli of different intensities is fundamental to pain perception, but its neural underpinnings are poorly understood. With neuroimaging techniques, Zhang et al. demonstrate that this ability is reliably and selectively encoded by pain-evoked brain responses, laying the foundation for objective pain assessment.

Zhang et al., 2022, Cell Reports Medicine 3, 100846
December 20, 2022
https://doi.org/10.1016/j.xcrm.2022.100846

CellPress

Cell Reports Medicine

CellPress
OPEN ACCESS

Article

Selective and replicable neuroimaging-based indicators of pain discriminability

Li-Bo Zhang,[1,2] Xue-Jing Lu,[1,2] Gan Huang,[3,4] Hui-Juan Zhang,[1,2] Yi-Heng Tu,[1,2] Ya-Zhuo Kong,[2,5] and Li Hu[1,2,6,*]
[1]CAS Key Laboratory of Mental Health, Institute of Psychology, Chinese Academy of Sciences, Beijing 100101, China
[2]Department of Psychology, University of Chinese Academy of Sciences, Beijing 100049, China
[3]School of Biomedical Engineering, Health Science Center, Shenzhen University, Shenzhen 518060, China
[4]Guangdong Provincial Key Laboratory of Biomedical Measurements and Ultrasound Imaging, Shenzhen University, Shenzhen 518060, China
[5]CAS Key Laboratory of Behavioral Science, Institute of Psychology, Chinese Academy of Sciences, Beijing 100101, China
[6]Lead contact
*Correspondence: huli@psych.ac.cn
https://doi.org/10.1016/j.xcrm.2022.100846

SUMMARY

Neural indicators of pain discriminability have far-reaching theoretical and clinical implications but have been largely overlooked previously. Here, to directly identify the neural basis of pain discriminability, we apply signal detection theory to three EEG (Datasets 1–3, total N = 366) and two fMRI (Datasets 4–5, total N = 399) datasets where participants receive transient stimuli of four sensory modalities (pain, touch, audition, and vision) and two intensities (high and low) and report perceptual ratings. Datasets 1 and 4 are used for exploration and others for validation. We find that most pain-evoked EEG and fMRI brain responses robustly encode pain discriminability, which is well replicated in validation datasets. The neural indicators are also pain selective since they cannot track tactile, auditory, or visual discriminability, even though perceptual ratings and sensory discriminability are well matched between modalities. Overall, we provide compelling evidence that pain-evoked brain responses can serve as replicable and selective neural indicators of pain discriminability.

INTRODUCTION

As typical signals for bodily dangers, painful stimuli need to be accurately distinguished. Mistaking an intense pain stimulus for a mild one can sometimes be life threatening. Previously, studies have examined how pain treatments affect the ability to discriminate between different painful stimuli,[1–5] how this pain discriminability differs between different groups (e.g., patients and healthy people),[6–9] and how brain activity responds differently to different noxious stimuli.[10–13] However, how the brain directly encodes pain discriminability has been overlooked almost entirely. Objective neural indicators of pain discriminability have profound theoretical and clinical implications, such as understanding pain processing in the brain and measuring pain discriminability in nonverbal individuals (e.g., comatose patients and infants).[14,15] Crucially, pain discriminability is of clear clinical relevance. Some chronic pain patients exhibit impaired pain discriminability,[16,17] and the improvement in chronic pain is related to increased pain discriminability.[18,19] However, assessing pain discriminability behaviorally can be unfeasible in certain individuals (e.g., those with cognitive-linguistic deficits) or undesirable in situations where the subjectivity and bias of pain reports cause deep concerns. Objective neural indicators that quantify pain discriminability using brain activity may thus be a valuable tool in the early screening and diagnosis of chronic pain and even help to develop pain-relieving treatments.

With the help of noninvasive neuroimaging techniques, such as electroencephalography (EEG) and functional magnetic resonance imaging (fMRI), previous studies have extensively investigated the functional representations of pain sensation.[20–25] Although pain-evoked brain responses (e.g., N2 and P2 components in event-related potentials [ERP]) and pain-related brain areas (e.g., insula, anterior cingulate cortex [ACC], and primary and secondary somatosensory cortices [S1, S2]) have been shown to differentially respond to noxious stimuli of various intensities,[10–13] neural responses that directly encode pain discriminability remain nearly unexplored.[26] Many vital questions are unanswered. First, it is unclear whether the neural activities that could be sampled using EEG and fMRI techniques reflect pain discriminability, that is, whether such neural activities directly correlate with pain discriminability across individuals, not just scale with stimulus intensity within individuals. Second, it is unknown whether the potential neural indicators of pain discriminability could be reliably identified in different situations, e.g., in different populations of participants. Finally, it is unclear whether the potential neural indicators are pain selective or not, that is, whether such neural responses selectively correlate with pain discriminability rather than sensory discriminability in general.

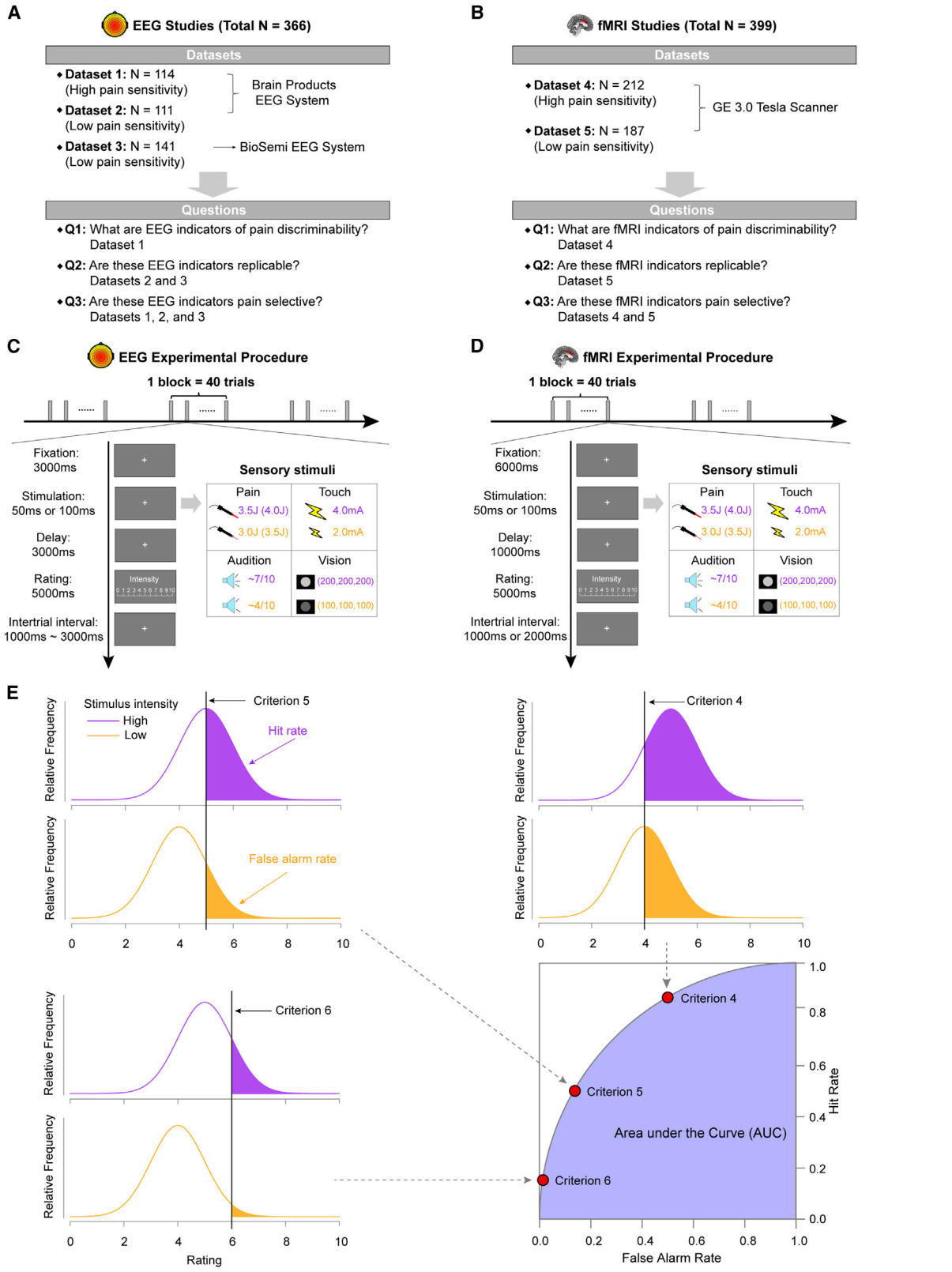

(legend on next page)

Here, we aimed to answer these questions by exploring neural indicators of pain discriminability using both EEG and fMRI techniques. We applied a signal detection theory (STD) approach to quantifying sensory discriminability on five large datasets (three EEG datasets [Datasets 1–3, total N = 366] and two fMRI datasets [Datasets 4–5, total N = 399]), in which Datasets 1 and 4 were used for exploration and others for validation. In each dataset, perceptual ratings and neural responses were collected when participants received transient stimuli of four sensory modalities (pain, touch, audition, and vision) and two intensities (high and low). With multiple independent datasets and multimodal sensory stimulations, we were able to not only reveal neural indicators of pain discriminability but also assess the replicability and pain selectivity of these neural indicators.

RESULTS

EEG indicators of pain discriminability

To identify EEG indicators of pain discriminability, we collected three large EEG datasets (N = 114, 111, and 141, respectively), in which painful laser, tactile, auditory, and visual stimuli of two intensities (high and low) were delivered to healthy participants (Figures 1A and 1C, see STAR Methods for details). Experimental details for collecting the three datasets were almost identical, except that data were collected from participants with different pain sensitivity (Dataset 1: high-pain-sensitivity participants receiving relatively low-energy laser stimuli [3.0 and 3.5 J]; Datasets 2 and 3: low-pain-sensitivity participants receiving relatively high-energy laser stimuli [3.5 and 4.0 J]) using different EEG devices (Datasets 1 and 2: Brain Products EEG system [BP]; Dataset 3: BioSemi EEG system).

Pain discriminability was quantified mainly using a nonparametric measure from SDT, i.e., the area under the receiver operating characteristic (ROC) curve (AUC) (Figure 1E; see STAR Methods for details on calculating AUC values).[27] As in many classic behavioral pain studies,[1–3,28] we adopted a rating design in terms of SDT, where participants simply rate the pain intensity of each stimulus on a numerical rating scale (NRS), and every rating on the NRS is regarded as an implicit criterion that participants hold.[29,30] We explored EEG responses correlated with pain discriminability using Dataset 1, replicated them in Datasets 2 and 3, and tested whether they are pain selective using all datasets with non-painful stimuli.

Pain stimuli can be distinguished in EEG datasets

Take Dataset 1 as an example: pain ratings evoked by high-intensity laser stimuli were significantly larger than those evoked by low-intensity laser stimuli (Figure 2A, $t(113) = 19.953$, $p < 0.0001$, Cohen's $d = 1.869$). This result suggested that participants were able to discriminate between the two noxious stimuli behaviorally. This observation was confirmed by AUC results. Across participants, the AUC values (0.804 ± 0.011) were significantly larger than chance level (i.e., 0.5; Figure 2A, $t(113) = 27.003$, $p < 0.0001$, Cohen's $d = 2.529$).

Similar to the behavioral results and consistent with many previous studies,[11,31,32] most brain responses evoked by nociceptive laser stimuli, such as the EEG deflections in the time domain (i.e., laser-evoked potentials, LEPs), encoded stimulus intensity. Specifically, high-intensity laser stimuli evoked larger N1, N2, and P2 waves than low-intensity stimuli (Figures 2B and S1A and Table S1, all p values < 0.0001). Event-related spectral perturbation, such as gamma-band event-related synchronization (γ-ERS), was also larger when elicited by high-intensity laser stimuli than low-intensity stimuli (Figures S2A and S2C and Table S1, $p = 0.0002$). Therefore, laser-elicited EEG responses could be used to distinguish between noxious stimuli of different intensities.

LEP responses are replicable indicators of pain discriminability

Significant correlations across participants were observed between the pain discriminability index (i.e., AUC) and differential LEP responses (amplitude differences between high-intensity and low-intensity laser stimuli) in Dataset 1: (1) N1, Pearson's $r = 0.448$, $p < 0.0001$; (2) N2, Pearson's $r = 0.547$, $p < 0.0001$; (3) P2, Pearson's $r = 0.434$, $p < 0.0001$ (Figure 2D and Table S2). These results were confirmed by a point-by-point correlation analysis, which showed that differential amplitudes at time points surrounding N1, N2, and P2 peaks were significantly correlated with AUC values (Figure 2C). Notably, their correlation coefficients were topographically distributed similarly to the corresponding LEP waves: the N1 wave was maximal over the central temporal region contralateral to the stimulated side, and N2 and P2 waves were more centrally distributed with a maximum at the vertex.

The robustness and replicability of the above findings were demonstrated from three different aspects. First, the correlation results were confirmed using different statistical strategies. On the one hand, nonparametric correlation analyses replicated the findings above (Table S2). On the other hand, Bayesian correlation analyses provided decisive evidence for these significant correlations: (1) N1, the Bayes factor (BF) for Pearson's $r = 2.614*10^4$; (2) N2, BF for Pearson's $r = 3.375*10^7$; and (3) P2, BF for Pearson's $r = 1.170*10^4$ (Figure 2D and Table S2). Second, the results obtained from Dataset 1 were fully replicated in Datasets 2 and 3 (see Figure 2D and Table S2 for statistical results), which indicated that the correlation results could be

Figure 1. Study design, experimental procedure, and discriminability index calculation

(A and B) EEG and fMRI study design. Consisting of five datasets with large sample sizes, the EEG and fMRI studies aimed to reveal neural indicators of pain discriminability and assess the replicability and selectivity of these neural indicators.

(C and D) EEG and fMRI experimental procedures. Participants were given transient stimuli belonging to four different sensory modalities (pain, touch, audition, and vision), each composed of two stimulus intensities (high and low, marked in purple and orange, respectively). After each stimulus, participants rated the perceived intensity, using a numerical rating scale ranging from 0 ("no sensation") to 10 ("the strongest sensation imaginable [in each stimulus modality]").

(E) A schematic diagram describing the calculation of the discriminability index, i.e., area under the curve (AUC). Eleven integral ratings (i.e., 0–11) on the rating scale can be treated as 11 implicit response criteria participants hold. For a given criterion (e.g., 5 in the top left plot), the hit rate and false alarm rate can be estimated to define a point on the receiver operating characteristic (ROC) curve (the bottom right plot). Eleven criteria define 11 points on the ROC, and the AUC value is defined as the area under the ROC curve.

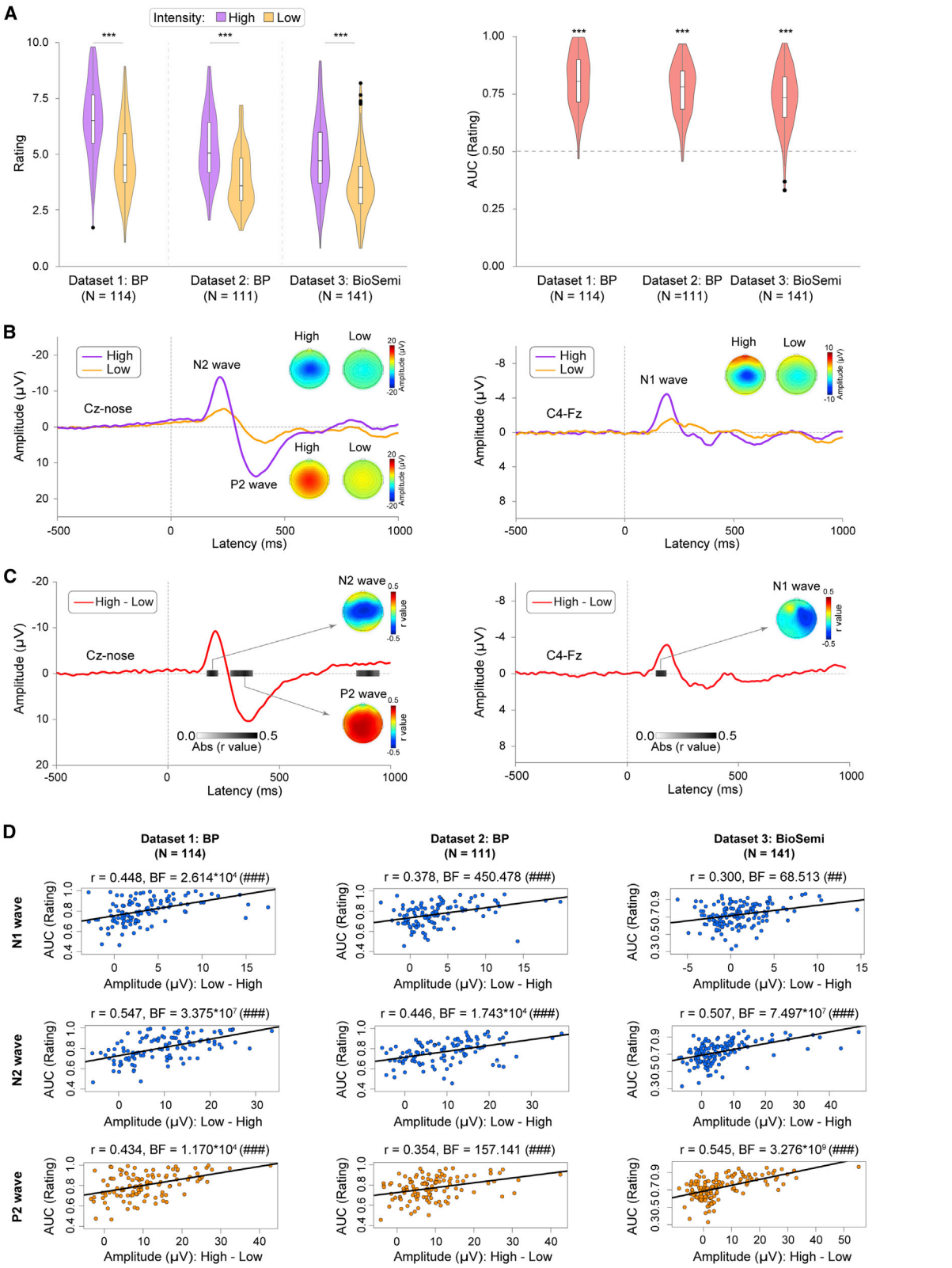

(legend on next page)

reliably observed in participants with different pain sensitivity and in independent datasets collected using different EEG systems. Third, the correlation results were replicated using two additional pain discriminability measures. Significant correlations were consistently observed between differential LEP responses and pain discriminability, regardless of whether pain discriminability was quantified using d′—a parametric measure from SDT—or simply the pain intensity rating difference between the high- and low-intensity conditions (see Figures S3B, S3C, S4B, and S4C and Tables S3 and S4).

Additional time-frequency analyses further confirmed the foregoing time domain findings. The time-frequency representations of LEP responses (Figure S2E, 100–350 ms and 1–20 Hz) also significantly correlated with pain AUC values. However, possibly due to a low signal-to-noise ratio, there was no consistent evidence for the significant correlation between γ-ERS magnitudes and AUC values. Only features in two small time-frequency regions around 300 ms and 50 Hz showed positive correlations with AUC values (Figure S2E).

In the three datasets analyzed above, the intensities of laser stimuli were either 3.0 vs. 3.5 J (Dataset 1) or 3.5 vs. 4.0 J (Datasets 2 and 3). To test whether the correlation between LEP responses and pain AUC values could be generalized to other intensity pairs, we reanalyzed another dataset (N = 95) from a study we published previously,[22] where participants received laser stimuli of four intensities, 2.5, 3.0, 3.5, and 4.0 J (see the original study[22] for experimental details). When the intensity difference was 0.5 J (i.e., 2.5 vs. 3.0 J, 3.0 vs. 3.5 J, and 3.5 vs. 4.0 J), LEP responses consistently correlated with pain AUC values (Table S5). However, the correlation became unstable when the intensity difference was 1.0 J (i.e., 2.5 vs. 3.5 J and 3.0 vs. 4.0 J), and they even disappeared when the intensity difference reached 1.5 J (i.e., 2.5 vs. 4.0 J) (Table S5). These results support the generalizability of our findings above, but also suggest that the robust correlation between LEP responses and pain discriminability may exist when the difference in stimulus intensity is within some appropriate range.

To assess the possibility of using LEP responses to quantify pain discriminability objectively, we trained a least absolute shrinkage and selection operator (LASSO) regression model[33] to continually predict AUC values using LEP responses in Dataset 1. Using LEP features (i.e., differences of peak amplitudes and latencies of N2 and P2 waves) at all electrodes, we found that the predicted AUC values showed a strong correlation with the real AUC values (Pearson's $r = 0.536$, $p < 0.0001$; see Figure S5). The generalizability of the model was demonstrated by the finding that this model could also predict pain AUC values in Dataset 2 (Pearson's $r = 0.423$, $p < 0.0001$; see Figure S5). This observation suggests a strong predictive power of LEP responses to quantify pain discriminability objectively and continually.

Our previous study showed that most LEP responses did not reflect pain sensitivity across participants.[22] This finding was replicated in the present study: no significant correlations were observed between mean N1 (Pearson's $r = 0.117$, $p = 0.215$, BF = 0.250), N2 (Pearson's $r = 0.016$, $p = 0.866$, BF = 0.119), and P2 amplitudes (Pearson's $r = 0.095$, $p = 0.317$, BF = 0.192) and mean pain ratings across participants (Figure S1B). Consequently, LEP responses do encode pain variability at the between-individual level, but their function is more related to pain discriminability than pain sensitivity.

LEP responses are selective indicators of pain discriminability

In line with pain perception, participants were able to behaviorally (Figure 3A) and neurophysiologically (Figures 3B and S6–S9 and Table S1) discriminate between high-intensity and low-intensity stimuli in all other sensory modalities. These observations were confirmed by AUC values in all sensory modalities, which were significantly larger than the chance level of 0.5 (see Figure 3A, minimal $t = 32.350$, maximal $p < 0.0001$, minimal Cohen's $d = 2.157$).

However, there was little evidence for significant correlations between differential tactile, auditory, or visual EEG responses and AUC values in Dataset 1&2 (Figures 3D and S7–S9 and Table S6). This finding was confirmed by point-by-point correlation analyses, as almost no time points showed significant correlations between differential ERP amplitudes and AUC values (Figure 3C). More evidence against the significant correlations was accumulated from three different aspects. First, no robust correlation results were obtained using different statistical strategies (Table S6). Notably, even though there were weak correlations between differential P2 amplitudes evoked by tactile (Pearson's $r = 0.176$) and auditory (Pearson's $r = 0.179$) stimuli and AUC values in Dataset 1&2 (Table S6), these correlations were significantly smaller than the correlation between differential P2 amplitudes evoked by laser stimuli and pain AUC values (Pearson's $r = 0.434$) in Dataset 1 (pain vs. touch: $Z = 2.469$, $p = 0.014$; pain vs. audition: $Z = 2.442$, $p = 0.015$). Second, similar results were obtained in Dataset 3 collected using the BioSemi EEG system (Figure 3E and Table S6), thus verifying the replicability of our findings in an independent dataset collected using different EEG devices. Third, when quantifying discriminability using d′ and intensity rating differences, no robust correlations were observed (Figures S3D–S3F and S4D–S4F and Tables S7 and S8). Note

Figure 2. Laser-evoked EEG responses reliably correlated with pain discriminability

(A) Distributions of pain ratings evoked by nociceptive laser stimuli of high (purple) and low (orange) intensities and distributions of pain AUC values. For all three datasets, pain ratings evoked by high-intensity stimuli were significantly greater than those evoked by low-intensity stimuli. AUC values in all datasets were significantly greater than the chance level of 0.5.

(B) The comparison of laser-evoked potentials (LEP) responses between high- and low-intensity stimuli in Dataset 1. Compared with low-intensity stimuli, high-intensity laser stimuli evoked larger N2/P2 (left) and N1 (right) waves.

(C) Point-by-point correlations between differential LEP responses (high–low) and AUC values in Dataset 1. Gray-shaded areas denote time intervals at which the amplitude differences (left: N2 and P2 waves; right: N1 wave) significantly correlated with AUC values (false discovery rate [FDR] corrected).

(D) Correlations between differential amplitudes of N1, N2, and P2 waves and AUC values. Differential N1, N2, and P2 amplitudes were consistently correlated with AUC values for all three datasets. ***$p < 0.001$; ##: Bayes factor (BF) > 10; ###: BF > 100. See Tables S1 and S2 for detailed statistical results.

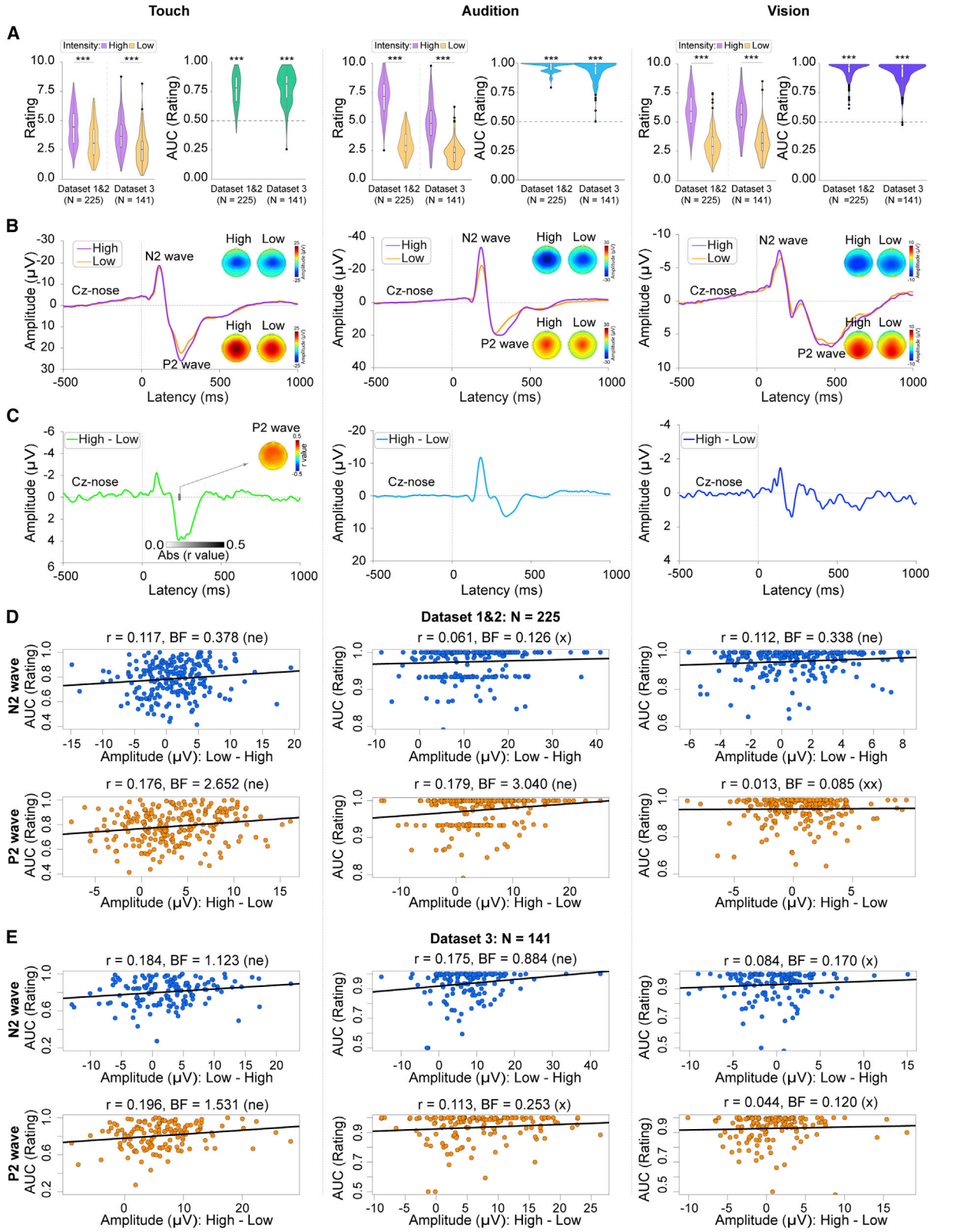

(legend on next page)

that d′ values (Figure S3A) were more normally distributed than AUC values (Figure 3A), and intensity rating differences showed few ceiling effects (Figure S4A). The congruent findings among the three discriminability measures suggest that the apparent ceiling effect of AUC values in auditory and visual modalities (Figure 3A) had little, if any, influence on our results.

Although we have provided strong evidence supporting that LEP responses selectively encode pain discriminability, one may still argue that the conclusion can be misleading as the perceptual intensity ratings were not strictly comparable between different sensory modalities (Figures 2A and 3A). To minimize the possible influence of rating differences between modalities, we adopted a matching procedure to equalize intensity ratings between pairs of sensory modalities (i.e., pain vs. touch, pain vs. audition, and pain vs. vision) (see STAR Methods for details of the matching algorithm). The matching procedure ensured that the intensity ratings were comparable between different sensory modalities (Figure 4). However, pain AUC values were significantly smaller than tactile, auditory, and visual AUC values (maximal $p = 0.024$), suggesting that participants were behaviorally better at discriminating between tactile, auditory, and visual stimuli of different intensities than painful stimuli (Figure 4). Despite this, significant correlations were always observed between differential LEP responses and pain AUC values (Figure 4, Tables S9 and S10), while no evidence supported the correlations between differential tactile, auditory, or visual EEG responses and their respective AUC values (Figure 4, Tables S11 and S12). Similar results were observed in Dataset 1&2 and Dataset 3, thus verifying that LEP responses selectively and reliably reflect pain discriminability.

We have provided evidence that the non-normal distributions of auditory and visual AUC values posed no serious problems for our findings. However, the seeming ceiling effect, even in the rating-matched data, may still cause some concerns. To address these concerns, we matched AUC values between modalities using all data in Datasets 1–3. The AUC matching ensured comparable AUC values between pain and other sensory modalities (Figure S10). However, we still observed that LEP responses consistently and robustly correlated with pain AUC values, whereas few ERP responses evoked by non-painful stimuli correlated with the corresponding AUC values (Figure S10, Tables S13 and S14). One may note that tactile P2 amplitudes significantly correlated with tactile AUC values after AUC matching. However, the correlation coefficient between tactile P2 amplitudes and AUC values (Pearson's $r = 0.229$) was significantly smaller than that between pain P2 amplitudes and AUC values (Pearson's $r = 0.479$; $Z = 2.985$, $p = 0.0028$). These findings suggest that the distribution of AUC values had little impact on our main conclusion that LEP responses selectively reflect pain discriminability.

The results above tested the selectivity of neural indicators of pain discriminability by correlating ERP responses in non-painful sensory modalities with the corresponding sensory discriminability. Another way to test it is to correlate LEP responses with sensory discriminability in non-painful modalities. Supporting the selective role of LEP responses in encoding pain discriminability, we found that LEP responses could not consistently correlate with tactile, auditory, and visual discriminability (Table S15). Furthermore, we tested whether the LASSO regression model trained using LEP responses in Dataset 1 could predict AUC values in other modalities in Dataset 1&2. Consistent with univariate correlation results, the trained model could not significantly predict tactile (Pearson's $r = 0.107$, $p = 0.1098$), auditory (Pearson's $r = 0.100$, $p = 0.1339$), or visual AUC values (Pearson's $r = 0.040$, $p = 0.5456$) (Figure S5).

Similar to previous studies,[22,34] we have mainly focused on vertex potentials in the above analyses, which are the most prominent deflections evoked by transient sensory stimuli.[35,36] However, focusing only on vertex potentials can be an important limitation in the present study. We thus conducted new control analyses to assess the possible relationship between other components (especially the early components) and sensory discriminability. We first re-referenced EEG signals to Fz to more accurately isolate early components[37–39] and then conducted point-by-point correlational analyses between the differential ERP waves (high–low) at all electrodes and AUC values for each sensory modality. It turned out that none of tactile, auditory, and visual ERPs at any electrode significantly correlated with the corresponding AUC values, while only LEPs showed significant correlations with pain AUC values within the time intervals of N1, N2, and P2 waves at a series of electrodes (Figure S11).

fMRI indicators of pain discriminability

To assess whether EEG findings on pain discriminability could be generalized to fMRI data, we collected two large fMRI datasets ($N = 212$ and 187, respectively), in which participants received stimuli of four sensory modalities (pain, touch, audition, and vision) and two intensities (high and low) in the MRI scanner (Figures 1B and 1D). Experimental details in the two datasets were almost identical, except that data were collected from participants with different pain sensitivity using different laser energies (Dataset 4: high-pain-sensitivity participants receiving relatively low-energy laser stimuli [3.0 and 3.5 J]; Dataset 5: low-pain-sensitivity participants receiving relatively high-energy laser stimuli [3.5 and 4.0 J]). We first examined possible

Figure 3. EEG responses evoked by tactile, auditory, and visual stimuli did not reflect their respective sensory discriminability

(A) Distributions of intensity ratings evoked by tactile (left), auditory (middle), and visual (right) stimuli of high (purple) and low (orange) intensities as well as distributions of sensory AUC values for each modality. For all three modalities, ratings evoked by high-intensity stimuli were significantly greater than those evoked by low-intensity stimuli, and AUC values were significantly greater than 0.5. Note that Datasets 1 and 2 were pooled together (Dataset 1&2) due to their identical experimental settings and stimulus parameters for the three modalities.

(B) The comparison of event-related potentials (ERP) responses between high- and low-intensity stimuli in Dataset 1&2.

(C) Point-by-point correlations between differential ERP responses and AUC values in Dataset 1&2. Only the differential amplitudes of P2 wave evoked by tactile stimuli weakly correlated with tactile AUC values (FDR corrected).

(D and E) Correlations between differential amplitudes of N2 and P2 waves and AUC values for different sensory modalities (D: Dataset 1&2; E: Dataset 3). For both datasets, no evidence showed that differential N2 and P2 amplitudes correlated with AUC values. ***$p < 0.001$; xx: $0.01 < BF < 0.1$; x: $0.1 < BF < 0.32$; ne: $0.32 < BF < 3.2$. See Tables S1 and S6 for detailed statistical results.

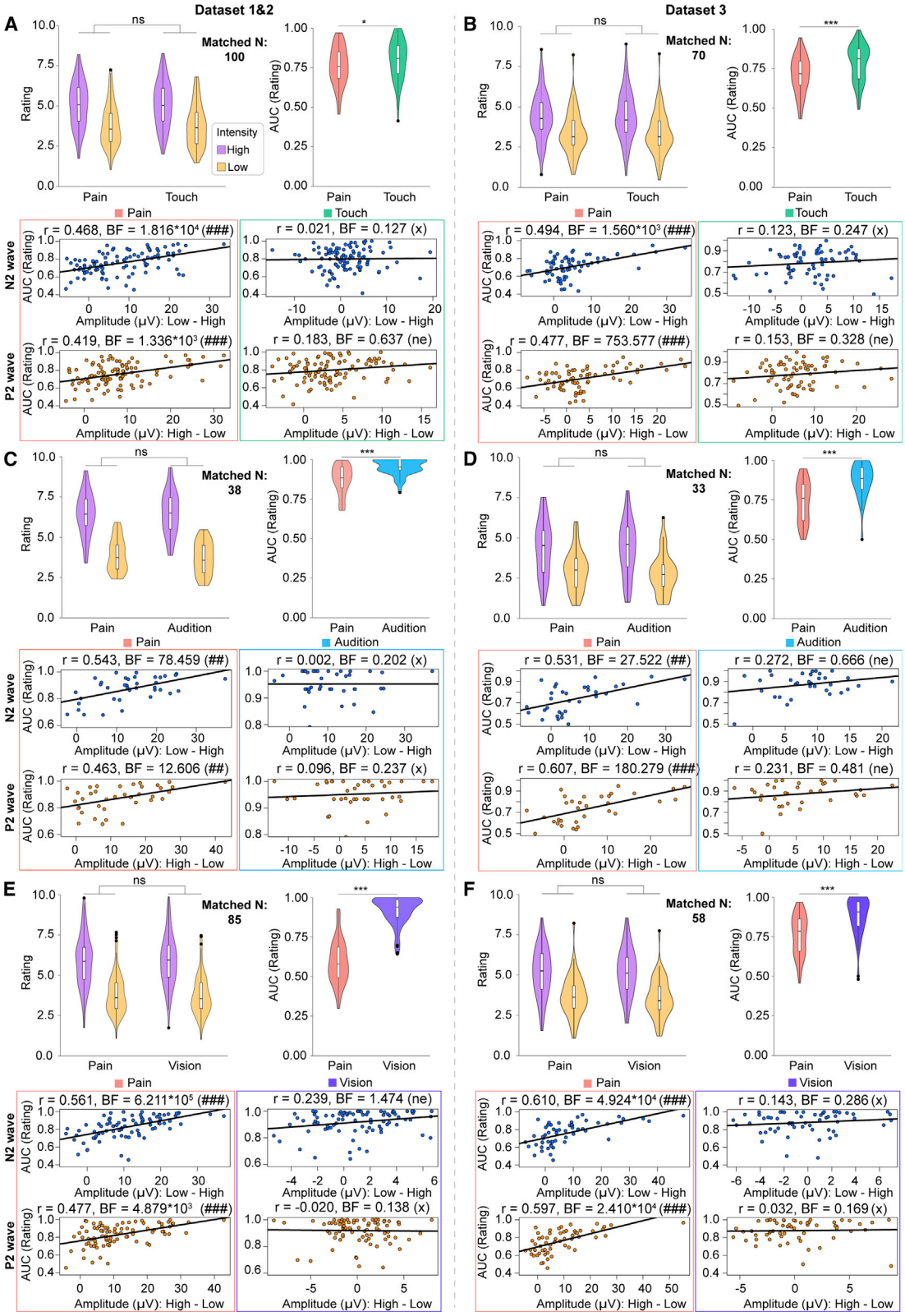

(legend on next page)

brain areas responsible for encoding pain discriminability using Dataset 4 and then replicated the findings using Dataset 5. Finally, we pooled both datasets to assess the pain-selectivity of the identified neural indicators.

Pain stimuli can be distinguished in fMRI datasets

In Dataset 4, pain ratings evoked by high-intensity laser stimuli were significantly higher than those evoked by low-intensity laser stimuli (Figure 5A, $t(211) = 18.830$, $p < 0.0001$, Cohen's $d = 1.293$), suggesting that participants could successfully discriminate between the two stimuli behaviorally. This finding was confirmed by the AUC values (0.714 ± 0.009), which were significantly larger than the chance level of 0.5 (Figure 5A, $t(211) = 23.752$, $p < 0.0001$, Cohen's $d = 1.631$).

Similar to EEG findings, laser-evoked neural responses sampled using the fMRI technique also encoded the stimulus intensity. Specifically, high-intensity laser stimuli led to stronger activations than low-intensity stimuli in a wide range of brain regions, including the thalamus, S1, S2, insula, and ACC (Figure 5B; family-wise error (FWE)-corrected $p < 0.05$ at the cluster level, the same hereinafter). In other words, brain regions whose neural responses are highly associated with pain processing[40–43] also contain information to distinguish noxious stimuli of different intensities.

Laser-evoked BOLD responses are replicable indicators of pain discriminability

In Dataset 4, significant positive correlations between differential blood-oxygen-level-dependent (BOLD) responses and pain AUC values were observed in the bilateral thalamus, S1, S2, insula, and some regions in ACC, cuneus, cerebellum, and so on (Figure 5B). In contrast, no brain areas showed significant negative correlations with pain AUC values. Notably, almost identical results were obtained when we assessed the correlations between differential BOLD responses and d' values as well as between differential BOLD responses and intensity rating differences (Figures S12B and S13B).

We then focused our analysis on brain regions associated with pain processing, namely, the bilateral thalamus, S1, S2, insula, and ACC. All of them had subareas significantly correlated with pain AUC values in Dataset 4 (Figure 5C). Defining these subareas as regions of interest (ROIs), we extracted their BOLD responses and correlated these responses with pain AUC values in Dataset 5 to assess the replicability of the findings in Dataset 4. There was substantial and robust evidence that BOLD responses in the left thalamus, left S1, left insula, and ACC were significantly correlated with pain AUC values (Figure 5C and Table S16). Moreover, there was also evidence, albeit weak, that BOLD responses in the right thalamus, right S1, and right insula were significantly correlated with pain AUC values (Table S16). Taken together, these results provided compelling evidence suggesting the replicability of fMRI indicators of pain discriminability.

To assess the possibility of using fMRI responses to quantify pain discriminability objectively, we trained a LASSO regression model[33] using first-level t maps of the contrast "high pain-low pain" in Dataset 4. The predicted AUC values showed a significant correlation with the real AUC values (Pearson's $r = 0.348$, $p < 0.0001$; see Figure S5). The trained model could also predict pain AUC values in Dataset 5 (Pearson's $r = 0.227$, $p = 0.0018$; see Figure S5), demonstrating its generalizability.

Laser-evoked BOLD responses are selective indicators of pain discriminability

In line with EEG findings, participants could also behaviorally and neurophysiologically discriminate between high-intensity and low-intensity stimuli in tactile, auditory, and visual modalities (Figure 6). Intensity ratings evoked by high-intensity stimuli were all significantly larger than those evoked by low-intensity stimuli (Figure 6A, minimal $t = 28.798$, maximal $p < 0.0001$, minimal Cohen's $d = 1.442$). Furthermore, AUC values in all sensory modalities were significantly larger than the chance level of 0.5 (Figure 6A, minimal $t = 37.573$, maximal $p < 0.0001$, minimal Cohen's $d = 1.881$). As compared with low-intensity stimuli, high-intensity tactile, auditory, and visual stimuli led to stronger activations in a wide range of brain areas, e.g., bilateral insula and ACC (Figures 6B–6D).

However, almost no brain regions showed significant correlations with tactile, auditory, or visual AUC values (Figures 6B–6D). The only exception was that, in the visual modality, a few areas in the occipital lobe (e.g., the middle occipital gyrus, lingual gyrus, and cuneus gyrus) correlated significantly with visual AUC values (Figure 6D). Notably, similar results were obtained when sensory discriminability was quantified using d' values and intensity rating differences, which, unlike AUC values, showed few ceiling effects (Figures S12 and S13).

As in the EEG studies, we also accounted for intensity rating differences across modalities using a matching procedure, which ensured that intensity ratings between different sensory modalities were equalized (Figure 7A). However, pain AUC values were significantly smaller than tactile, auditory, and visual AUC values (maximal $p = 0.002$, Figure 7A). Despite this, significant correlations were observed between differential laser-evoked BOLD responses in the foregoing pain-related brain regions and pain AUC values, while almost no brain regions showed significant correlations between differential tactile, auditory, or visual BOLD responses and their respective AUC values (Figures 7B–7D).

We also tested the selectivity of fMRI-based neural indicators of pain discriminability by correlating laser-evoked fMRI signals with sensory discriminability in non-painful modalities. Almost no cluster correlated significantly with tactile, auditory, or visual

Figure 4. The selectivity of EEG indicators of pain discriminability

(A and B) N2 and P2 selectively correlated with pain discriminability after pain and tactile intensity ratings were matched. For both Dataset 1&2 (A) and Dataset 3 (B), the matching procedure equalized ratings for pain and touch, although pain AUC values were significantly smaller than tactile AUC values. Notably, for both Dataset 1&2 and Dataset 3, differential N2 and P2 amplitudes evoked by noxious laser stimuli correlated with pain AUC values. However, no evidence could be obtained in favor of the correlation between differential N2 and P2 amplitudes and tactile AUC values.

(C and D) N2 and P2 selectively correlated with pain discriminability after pain and auditory intensity ratings were matched.

(E and F) N2 and P2 selectively correlated with pain discriminability after pain and visual intensity ratings were matched. *$0.01 < p < 0.05$; ***$p < 0.001$; ns: $p > 0.05$; x: $0.1 < BF < 0.32$; ne: $0.32 < BF < 3.2$; ##: $10 < BF < 100$; ###: $BF > 100$. See Tables S9–S12 for detailed statistical results.

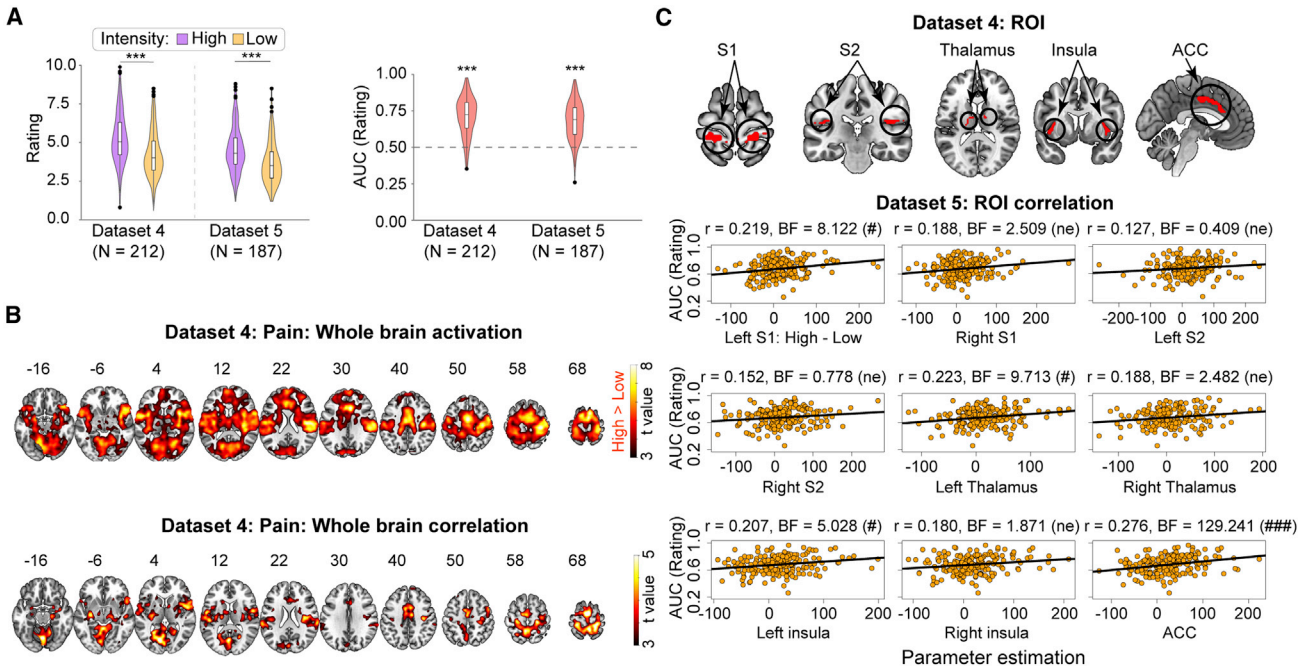

Figure 5. Laser-evoked fMRI responses reliably correlated with pain discriminability

(A) Distributions of pain ratings evoked by nociceptive laser stimuli of high (purple) and low (orange) intensities and distributions of pain AUC values. For both datasets, pain ratings evoked by high-intensity stimuli were significantly greater than those evoked by low-intensity stimuli. AUC values in both datasets were significantly greater than 0.5.

(B) Brain regions showed stronger activation by high-intensity stimuli than low-intensity stimuli (top), and brain regions showed significant correlations between their differential blood-oxygen-level-dependent (BOLD) responses and AUC values (bottom) in Dataset 4.

(C) Pain-related regions of interests (ROIs), defined according to the correlation results in Dataset 4, including the bilateral S1, S2, thalamus, insula, and ACC. Differential BOLD responses in several pain-related ROIs (i.e., left S1, left thalamus, left insula, and ACC) also strongly correlated with AUC values in Dataset 5, thus verifying the replicability of the findings obtained in Dataset 4. For whole brain analyses, the significance threshold was set at $p = 0.001$ at the voxel level and $p_{FWE} = 0.05$ at the cluster level. ***$p < 0.001$; ne: $0.32 < BF < 3.2$; #: $3.2 < BF < 10$; ###: $BF > 100$. See Table S16 for detailed statistical results.

AUC values (Figure S14). Furthermore, the LASSO regression model that significantly predicted pain AUC values failed to predict tactile (Pearson's $r = -0.010$, $p = 0.8415$), auditory (Pearson's $r = 0.003$, $p = 0.9452$), or visual AUC values (Pearson's $r = -0.019$, $p = 0.7061$) (Figure S5). Collectively, our findings suggest that BOLD responses evoked by nociceptive laser stimuli selectively reflect pain discriminability.

DISCUSSION

Quantifying pain discriminability mainly using SDT-derived measures in five large datasets (two exploration datasets and three validation datasets), we found that brain responses evoked by painful laser stimuli reliably correlated with pain discriminability, while almost no significant correlations were observed between brain responses and sensory discriminability in tactile, auditory, and visual modalities. These observations were well replicated and validated using different statistical strategies and discriminability indices in independent datasets sampled using different techniques (i.e., EEG and fMRI) and devices (i.e., BP and BioSemi EEG systems). Moreover, the observations could be generalized to participants with different pain sensitivity and settings with different stimulus parameters. Crucially, the neural indicators of pain discriminability were pain selective since the brain responses could not track the sensory discriminability in tactile, auditory, and visual modalities, even though perceptual ratings and AUC values were well matched between modalities. Altogether, we provided compelling evidence that most EEG (i.e., N1, N2, and P2 amplitudes) and fMRI brain responses (e.g., BOLD activations in the thalamus, S1, insula, and ACC) evoked by painful laser stimuli are replicable and selective neural indicators of pain discriminability.

Brain responses evoked by noxious stimuli reliably encode pain discriminability

In previous EEG and fMRI studies, the majority of brain responses elicited by transient noxious stimuli reflect pain perception at the within-individual level,[20,44–47] but they fail to reflect the pain variability across individulas.[22,48] Consequently, these brain responses do not reflect pain-specific neural activity, but rather they reflect other physiological outcomes of the arrival of the transient nociceptive volley to the cortex besides pain, such as autonomic responses and motor responses.[49–51] Notably, all these observations and subsequent interpretations were derived in the framework of pain sensitivity—the ability to perceive the same noxious stimulus as more (or less) painful than others—both at the within-individual and between-individual levels. Moving beyond this traditional framework, we explored neural

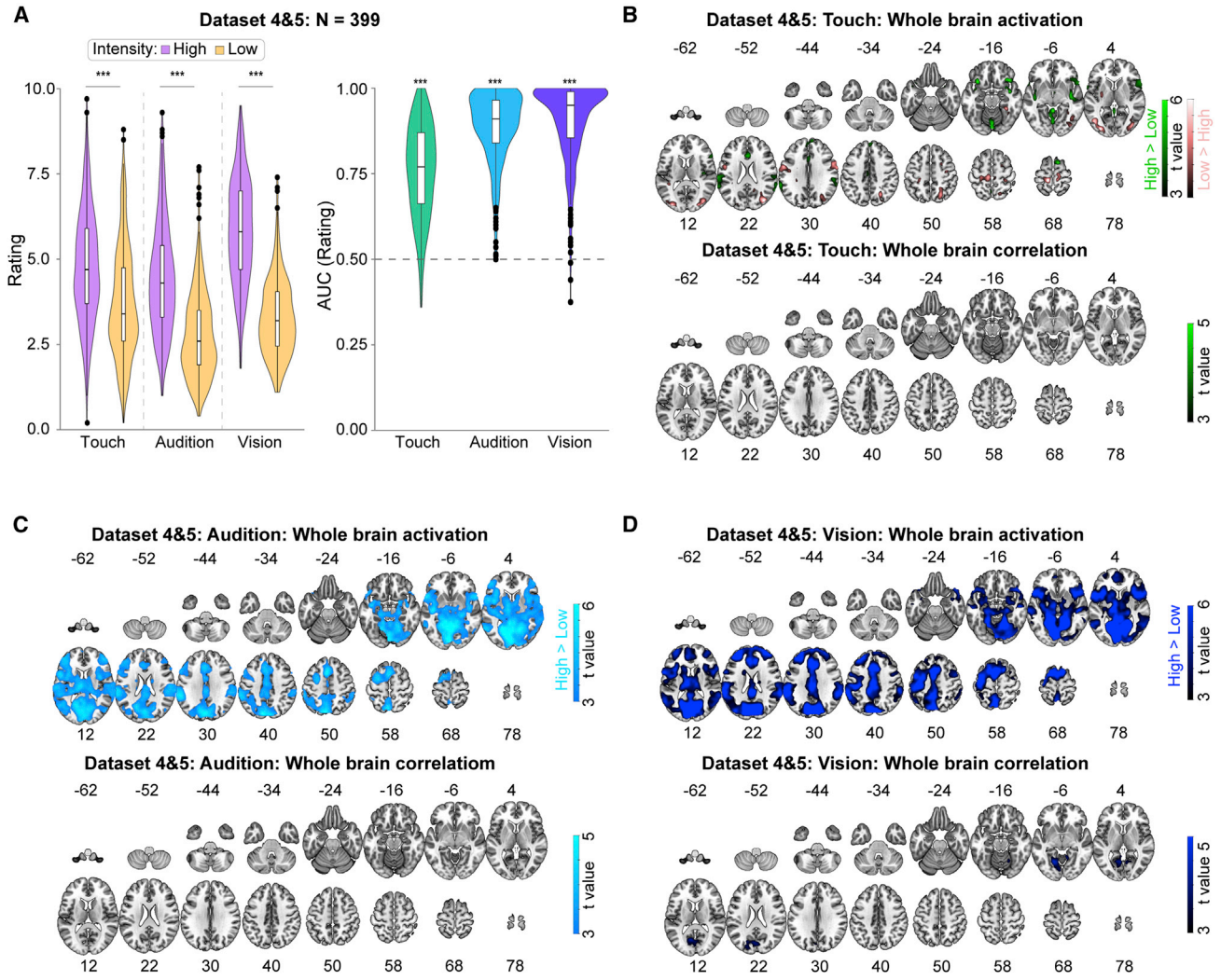

Figure 6. fMRI responses evoked by tactile, auditory, and visual stimuli did not reflect their respective sensory discriminability

(A) Distributions of intensity ratings evoked by tactile (left), auditory (middle), and visual (right) stimuli of high (purple) and low (orange) intensities as well as distributions of sensory AUC values for each modality. For all three modalities, ratings evoked by high-intensity stimuli were significantly greater than those evoked by low-intensity stimuli, and AUC values were significantly greater than 0.5. Note that Datasets 4 and 5 were pooled together due to their identical experimental settings and stimulus parameters for the three modalities.

(B–D) Brain regions showed stronger activation by high-intensity stimuli than low-intensity stimuli (top), and brain regions showed significant correlations between their differential BOLD responses and AUC values for each sensory modality (bottom). Although tactile (B), auditory (C), and visual (D) stimuli of high intensity evoked stronger activations in a series of brain regions (e.g., bilateral insula and ACC) than low-intensity stimuli, almost no brain regions showed significant correlations with AUC values. The only exception was that, for the visual modality, some areas in the occipital cortex correlated significantly with visual AUC values. ***$p < 0.001$.

indicators of pain discriminability: the ability to distinguish painful stimuli of different intensities. Extending a previous preliminary study showing significant correlations between LEPs and pain discriminability,[26] we provided solid evidence that the majority of EEG and fMRI brain responses elicited by nociceptive laser stimuli consistently reflect the variability in pain discriminability across participants. The replicability of the discovered neural indicators was demonstrated using different statistical strategies and discriminability indices in five large datasets (all Ns > 100) sampled by different techniques (i.e., EEG and fMRI) and devices. Importantly, results from EEG datasets agreed well with those from fMRI datasets, considering that N1, N2, and P2 waves in LEPs are mainly generated from the S1, S2, insula, and ACC,[52,53] whose activities also encoded pain discriminability. These findings introduce a reinterpretation of the majority of brain responses evoked by transient noxious stimuli. They could reflect the ability of an individual to discriminate between different transient noxious stimuli. Moreover, machine learning results showed that laser-evoked brain responses could be used to accurately predict pain discriminability for a given individual. Therefore, we could evaluate pain discriminability objectively using laser-evoked brain responses only (i.e., without the

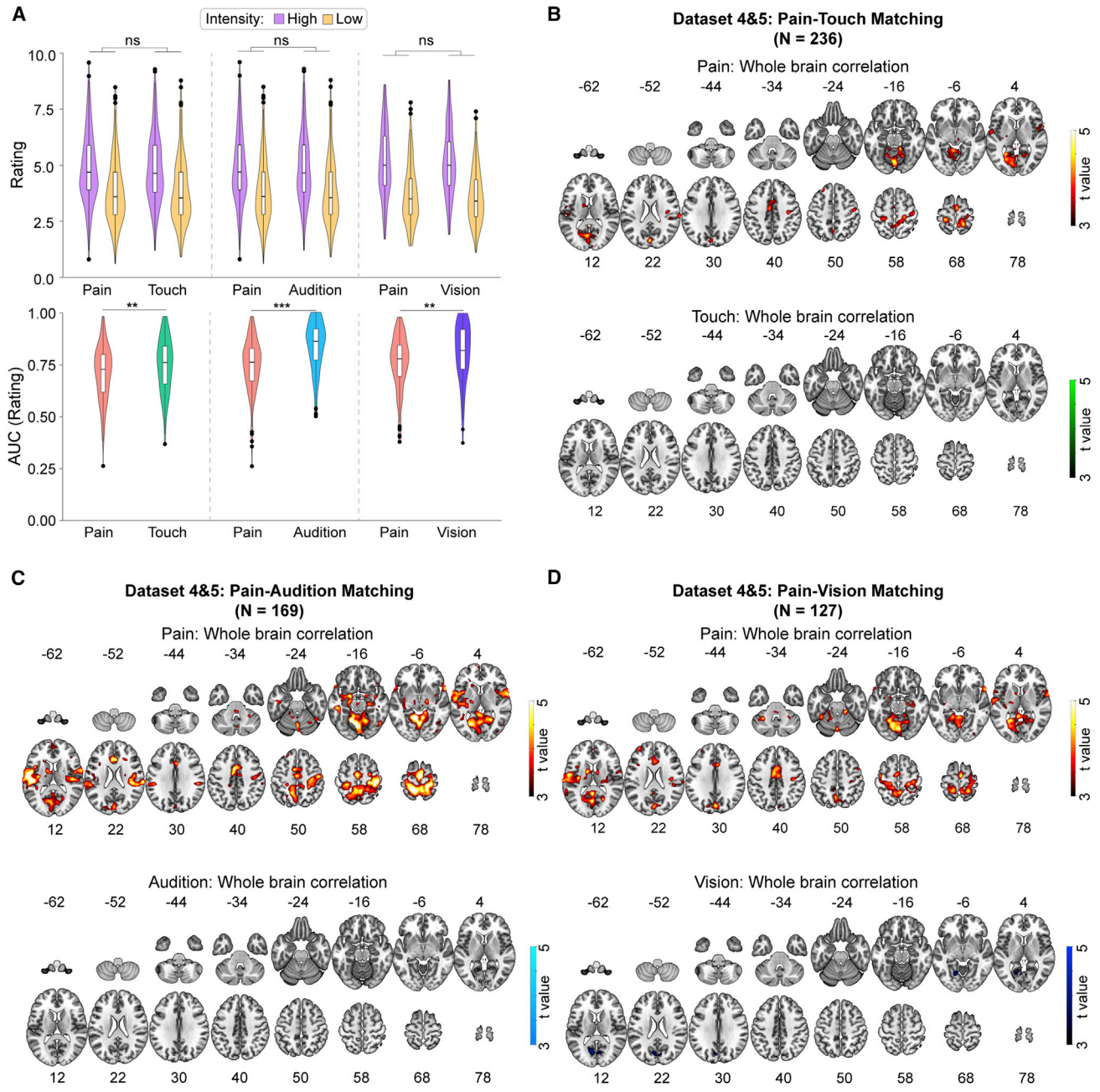

Figure 7. The selectivity of fMRI indicators of pain discriminability

(A) Distributions of intensity ratings and AUC values of pain and a non-pain sensation after their ratings were matched (left: pain vs. touch; middle: pain vs. audition; right: pain vs. vision). The matching procedure equalized ratings for each pair of sensory modalities. However, pain AUC values were significantly smaller than non-pain AUC values for all comparisons.

(B–D) Brain regions showed significant correlations between differential BOLD responses and AUC values after pain ratings were matched with tactile (B), auditory (C), and visual (D) intensity ratings. For all comparisons, differential BOLD responses evoked by nociceptive laser stimuli significantly correlated with pain AUC values, while almost no significant correlations were observed for the three non-painful sensory modalities. Only a few areas in the occipital cortex significantly correlated with visual AUC values for the visual modality. ***$p < 0.001$; **$0.001 < p < 0.01$; ns: $p > 0.05$.

requirement of collecting subjective pain ratings), which would greatly extend the applications of these brain responses in clinical practice, such as the development of new pain therapeutics.

Brain responses evoked by noxious stimuli selectively encode pain discriminability

In contrast to brain responses evoked by painful laser stimuli that reliably correlated with pain discriminability, almost no

significant correlations were observed between brain responses evoked by tactile, auditory, and visual stimuli and their respective sensory discriminability, even though participants could discriminate between stimuli of different intensities behaviorally and neurophysiologically in these sensory modalities. These findings were also highly replicable, as similar results were obtained using different statistical methods and discriminability indices in independent datasets. Most importantly, consistent results were obtained even when a rating matching procedure was adopted to equalize perceptual ratings between different sensory modalities, thus eliminating the possible influence of rating differences between modalities on our findings. These results were also replicated when using discriminability measures (i.e., d′ and intensity rating difference) that showed few ceiling effects and when manually matching AUC values between modalities, thus effectively ruling out the influence of AUC distributions on our findings. Taken together, the relationship between neural responses evoked by transient noxious stimuli and pain discriminability is probably pain selective.

These findings appear, at first glance, not in accord with previous studies, which showed that the majority of brain responses evoked by nociceptive laser stimuli do not represent an obligatory pain signature but are highly associated with stimulus salience.[54–58] This interpretation is mainly driven by the fact that similar neural responses can also be evoked by equally salient but non-painful tactile, auditory, or visual stimuli.[34,55,57] Given that these multimodal neural activities are also activated in situations where no pain is present, it is an incorrect reverse inference to conclude that they represent an obligatory pain signature.[14,59] In the present study, whereas no evidence showed that neural responses evoked by non-painful tactile, auditory, or visual stimuli could reflect their corresponding sensory discriminability, neural responses evoked by painful laser stimuli reliably encoded pain discriminability. However, previous studies have mainly focused on whether brain responses evoked by nociceptive laser stimuli selectively reflect pain sensitivity. Bear in mind that pain discriminability is distinct from pain sensitivity, and these two concepts can be independent. One can have a high pain sensitivity, yet simultaneously have a low pain discriminability. For example, one may rate a nociceptive laser stimulus of 2.0 J as 7.5 on the 0–10 NRS and another stimulus of 2.5 J as 7.6. This person is presumably highly pain-sensitive but can hardly discriminate between the two stimuli. Consequently, our findings and previous ones are not really inconsistent. Instead, their seeming inconsistency highlights an essential but frequently ignored discriminative function of transient pain-evoked brain responses. In agreement with our findings, Beck et al. also showed that the correlations between stimulus-evoked brain responses and discriminability values were larger in pain than in touch.[26]

Why do brain responses selectively encode pain discriminability?

The finding that pain discriminability is selectively encoded by laser-evoked brain responses begs a thorny question: why does the neural processing of pain discriminability differ from the discriminability of other sensory modalities? One possibility is that discriminability is simply more important for pain perception. In real life, intensity discriminability is a predominant function of pain perception. In contrast, touch, audition, and vision encode plentiful information other than intensity, for example, texture and humidity for touch, timbre and pitch for audition, color and shape for vision. Discriminating painful stimuli also seems to have a more significant survival value, as mistaking an intense pain stimulus for a mild one can sometimes be life threatening. The importance of pain discriminability may warrant the nervous system selectively encoding this information, perhaps starting from the early stage of pain processing. Indeed, we observed significant correlations between pain discriminability and the earliest part of the neural responses sampled using EEG (N1 wave in LEPs[60]) and fMRI (BOLD responses in the thalamus[61]) techniques.

However, this interpretation cannot easily explain the finding that the significant correlation between brain activity and pain discriminability became unstable or even disappeared when the intensity differences in the two painful stimuli reached 1.0 J or larger. This observation is theoretically reasonable. Suppose that we had delivered stimuli with extremely large intensity differences (e.g., 2.0 and 5.0 J). It would be nearly impossible for brain responses to correlate with pain discriminability, since all healthy participants would be perfectly able to distinguish these two stimuli (i.e., AUC = 1 for all participants). Moreover, we observed that pain AUC values were consistently smaller than tactile, auditory, and visual AUC values even after intensity ratings were carefully matched between modalities. This observation is in agreement with many psychophysical studies showing that humans have superb sensory discriminability in non-painful modalities.[62–65] For example, human eyes can even discriminate between one and two photons.[66] Our findings can thus be restated as showing that the brain contains little information about discriminability when stimuli can be trivially discriminated (as in touch, audition, and vision, or pain when intensity differences are large), as cortical processing may be unnecessary in such a trivial task. Instead, the task can be achieved in the brainstem or at the spiral cord level.[67–69] On the contrary, when the discrimination requires more effort (as in pain when intensity differences are not so large), the conscious perceptual processing in the cortex may be required, since higher cognitive processes like decision-making may be involved in completing the difficult task. Future studies are needed to explore the reasons for the observation that pain discriminability is selectively encoded in the brain and to empirically test all possible interpretations.

Limitations of the study

The limitation of the present study is that we did not collect clinical data to assess the clinical applicability of the neural indicators of pain discriminability we discovered. Our findings that brain responses evoked by painful laser stimuli can serve as objective measures of pain discriminability may have far-reaching clinical implications. Objectively assessing pain discriminability based on neural responses would be eminently desirable in specific clinical populations, such as non-communicative patients and patients with disorders of consciousness. Notably, previous studies have reported that some chronic pain patients (e.g., low back pain patients) have impaired pain discriminability,[16,17] and the improvement in chronic pain is associated with

better pain discriminability.[18,19] Furthermore, sensory discrimination training has been shown to reduce pain and reverse cortical reorganization caused by chronic pain.[70,71] Therefore, the availability of a physiological and objective assessment of pain discriminability may also be helpful in the early screening and diagnosis of chronic pain and the development of individual-specific strategies for pain-relieving treatments.

To realize these potential clinical applications, future clinical studies should be performed in at least two aspects. First, it would be necessary to test the impact of chronic pain on the neural indicators of pain discriminability. If these neural indicators are implicated in chronic pain, pathological alterations of these brain responses may prove beneficial for early objective screening and diagnosis of chronic pain. Second, it would be interesting to examine the role of these neural indicators in pain-relieving effects of discrimination training. Future studies may target these neural indicators using individual-based neural modulation techniques to alleviate suffering for chronic pain patients.

STAR★METHODS

Detailed methods are provided in the online version of this paper and include the following:

- KEY RESOURCES TABLE
- RESOURCE AVAILABILITY
  - Lead contact
  - Materials availability
  - Data and code availability
- EXPERIMENTAL MODEL AND SUBJECT DETAILS
- METHOD DETAILS
  - EEG studies
  - fMRI studies
- QUANTIFICATION AND STATISTICAL ANALYSIS
  - EEG studies
  - fMRI studies

SUPPLEMENTAL INFORMATION

Supplemental information can be found online at https://doi.org/10.1016/j.xcrm.2022.100846.

ACKNOWLEDGMENTS

We wish to thank Prof. Giandomenico Iannetti for his insightful comments on the manuscript and Prof. Meng Liang for his valuable help in the rating and AUC matching algorithm. L.H. is supported by the National Natural Science Foundation of China (32071061, 31822025) and Beijing Natural Science Foundation (JQ22018). X.J.L. is supported by the National Natural Science Foundation of China (32171077). Y.H.T. is supported by the "Sci-Tech Innovation 2030" Brain Science and Brain-Inspired Intelligence Technology Research by the Ministry of Science and Technology of the People's Republic of China (2022ZD0206400). L.H., X.J.L., Y.H.T., and Y.Z.K. are supported by the Scientific Foundation of Institute of Psychology, Chinese Academy of Sciences (E2CX4015).

AUTHOR CONTRIBUTIONS

Conceptualization: L.B.Z., L.H., and X.J.L. Methodology: L.H., L.B.Z., and X.J.L. Investigation: H.J.Z. and L.B.Z. Formal analysis: L.B.Z. and G.H. Writing – original draft: L.B.Z. Writing – review & editing: L.H., L.B.Z., Y.H.T., Y.Z.K., and X.J.L. Visualization: Z.L.B. and L.H. Funding acquisition: L.H., X.J.L., T.H.Y., and Y.Z.K. Project administration: L.H. Supervision: L.H.

DECLARATION OF INTERESTS

The authors declare no competing interests.

Received: June 25, 2022
Revised: September 18, 2022
Accepted: November 9, 2022
Published: December 5, 2022

REFERENCES

1. Chapman, C.R., Murphy, T.M., and Butler, S.H. (1973). Analgesic strength of 33 percent nitrous oxide: a signal detection theory evaluation. Science *179*, 1246–1248. https://doi.org/10.1126/science.179.4079.1246.
2. Clark, W.C. (1969). Sensory-decision theory analysis of the placebo effect on the criterion for pain and thermal sensitivity (d'). J. Abnorm. Psychol. *74*, 363–371.
3. Clark, W.C., and Yang, J.C. (1974). Acupunctural analgesia? Evaluation by signal detection theory. Science *184*, 1096–1098.
4. Mancini, F., Nash, T., Iannetti, G.D., and Haggard, P. (2014). Pain relief by touch: a quantitative approach. Pain *155*, 635–642. https://doi.org/10.1016/j.pain.2013.12.024.
5. Valmunen, T., Pertovaara, A., Taiminen, T., Virtanen, A., Parkkola, R., and Jääskeläinen, S.K. (2009). Modulation of facial sensitivity by navigated rTMS in healthy subjects. Pain *142*, 149–158. https://doi.org/10.1016/j.pain.2008.12.031.
6. Dorn, S.D., Palsson, O.S., Thiwan, S.I.M., Kanazawa, M., Clark, W.C., van Tilburg, M.A.L., Drossman, D.A., Scarlett, Y., Levy, R.L., Ringel, Y., et al. (2007). Increased colonic pain sensitivity in irritable bowel syndrome is the result of an increased tendency to report pain rather than increased neurosensory sensitivity. Gut *56*, 1202–1209. https://doi.org/10.1136/gut.2006.117390.
7. Janal, M.N., Glusman, M., Kuhl, J.P., and Clark, W.C. (1994). Are runners stoical? An examination of pain sensitivity in habitual runners and normally active controls. Pain *58*, 109–116. https://doi.org/10.1016/0304-3959(94)90190-2.
8. Kowalczyk, W.J., Sullivan, M.A., Evans, S.M., Bisaga, A.M., Vosburg, S.K., and Comer, S.D. (2010). Sex differences and hormonal influences on response to mechanical pressure pain in humans. J. Pain *11*, 330–342. https://doi.org/10.1016/j.jpain.2009.08.004.
9. Slimani, H., Ptito, M., and Kupers, R. (2015). Enhanced heat discrimination in congenital blindness. Behav. Brain Res. *283*, 233–237. https://doi.org/10.1016/j.bbr.2015.01.037.
10. Frot, M., Magnin, M., Mauguière, F., and Garcia-Larrea, L. (2007). Human SII and posterior insula differently encode thermal laser stimuli. Cereb. Cortex *17*, 610–620. https://doi.org/10.1093/cercor/bhk007.
11. Hu, L., Cai, M.M., Xiao, P., Luo, F., and Iannetti, G.D. (2014). Human brain responses to concomitant stimulation of Aδ and C nociceptors. J. Neurosci. *34*, 11439–11451.
12. Ohara, S., Crone, E.N., Weiss, N., Treede, R.D., and Lenz, A.F. (2004). Amplitudes of laser evoked potential recorded from primary somatosensory, parasylvian and medial frontal cortex are graded with stimulus intensity. Pain *110*, 318–328. https://doi.org/10.1016/j.pain.2004.04.009.
13. Timmermann, L., Ploner, M., Haucke, K., Schmitz, F., Baltissen, R., and Schnitzler, A. (2001). Differential coding of pain intensity in the human primary and secondary somatosensory cortex. J. Neurophysiol. *86*, 1499–1503. https://doi.org/10.1152/jn.2001.86.3.1499.
14. Mouraux, A., and Iannetti, G.D. (2018). The search for pain biomarkers in the human brain. Brain *141*, 3290–3307. https://doi.org/10.1093/brain/awy281.

15. Tracey, I. (2021). Neuroimaging enters the pain biomarker arena. Sci. Transl. Med. *13*, eabj7358. https://doi.org/10.1126/scitranslmed.abj7358.

16. Cohen, M.J., Naliboff, B.D., Schandler, S.L., and Heinrich, R.L. (1983). Signal detection and threshold measures to loud tones and radiant heat in chronic low back pain patients and cohort controls. Pain *16*, 245–252. https://doi.org/10.1016/0304-3959(83)90112-4.

17. Naliboff, B.D., Cohen, M.J., Schandler, S.L., and Heinrich, R.L. (1981). Signal detection and threshold measures for chronic back pain patients, chronic illness patients, and cohort controls to radiant heat stimuli. J. Abnorm. Psychol. *90*, 271–274.

18. Malow, R.M., and Olson, R.E. (1981). Changes in pain perception after treatment for chronic pain. Pain *11*, 65–72. https://doi.org/10.1016/0304-3959(81)90139-1.

19. Yang, J.C., Clark, W.C., and Janal, M.N. (1991). Sensory decision theory and visual analogue scale indices predict status of chronic pain patients six months later. J. Pain Symptom Manag. *6*, 58–64. https://doi.org/10.1016/0885-3924(91)90519-A.

20. Coghill, R.C., Sang, C.N., Maisog, J.M., and Iadarola, M.J. (1999). Pain intensity processing within the human brain: a bilateral, distributed mechanism. J. Neurophysiol. *82*, 1934–1943. https://doi.org/10.1152/jn.1999.82.4.1934.

21. Gross, J., Schnitzler, A., Timmermann, L., and Ploner, M. (2007). Gamma oscillations in human primary somatosensory cortex reflect pain perception. PLoS Biol. *5*, e133. https://doi.org/10.1371/journal.pbio.0050133.

22. Hu, L., and Iannetti, G.D. (2019). Neural indicators of perceptual variability of pain across species. Proc. Natl. Acad. Sci. *116*, 1782–1791. https://doi.org/10.1073/pnas.1812499116.

23. Huang, G., Xiao, P., Hung, Y.S., Iannetti, G.D., Zhang, Z.G., and Hu, L. (2013). A novel approach to predict subjective pain perception from single-trial laser-evoked potentials. Neuroimage *81*, 283–293. https://doi.org/10.1016/j.neuroimage.2013.05.017.

24. Liang, M., Su, Q., Mouraux, A., and Iannetti, G.D. (2019). Spatial patterns of brain activity preferentially reflecting transient pain and stimulus intensity. Cereb. Cortex *29*, 2211–2227. https://doi.org/10.1093/cercor/bhz026.

25. Wager, T.D., Atlas, L.Y., Lindquist, M.A., Roy, M., Woo, C.W., and Kross, E. (2013). An fMRI-based neurologic signature of physical pain. N. Engl. J. Med. *368*, 1388–1397.

26. Beck, B., Cook, S., Iannetti, G.D., and Haggard, P. (2019). Neural markers of nociceptive input and pain intensity coding: a signal detection approach. Preprint at PsyArXiv. https://doi.org/10.31234/osf.io/dxeyn.

27. McNicol, D. (2016). A Primer of Signal Detection Theory (Lawrence Erlbaum Associates).

28. Chapman, C.R., Chen, A.C., and Bonica, J.J. (1977). Effects of intrasegmental electrical acupuncture on dental pain: evaluation by threshold estimation and sensory decision theory. Pain *3*, 213–227. https://doi.org/10.1016/0304-3959(77)90003-3.

29. Macmillan, N.A. (2002). Signal detection theory. In Stevens' Handbook of Experimental Psychology, J. Wixted, ed. (John Wiley & Sons).

30. Rollman, G.B. (1977). Signal detection theory measurement of pain: a review and critique. Pain *3*, 187–211.

31. Carmon, A., Mor, J., and Goldberg, J. (1976). Evoked cerebral responses to noxious thermal stimuli in humans. Exp. Brain Res. *25*, 103–107. https://doi.org/10.1007/BF00237330.

32. Zhang, Z.G., Hu, L., Hung, Y.S., Mouraux, A., and Iannetti, G.D. (2012). Gamma-band oscillations in the primary somatosensory cortex—a direct and obligatory correlate of subjective pain intensity. J. Neurosci. *32*, 7429–7438.

33. Tibshirani, R. (1996). Regression shrinkage and selection via the Lasso. J. R. Stat. Soc. Ser. B Methodol. *58*, 267–288. https://doi.org/10.1111/j.2517-6161.1996.tb02080.x.

34. Mouraux, A., and Iannetti, G.D. (2009). Nociceptive laser-evoked brain potentials do not reflect nociceptive-specific neural activity. J. Neurophysiol. *101*, 3258–3269.

35. Walter, W.G. (1964). The convergence and interaction of visual, auditory, and tactile responses in human nonspecific cortex. Ann. N. Y. Acad. Sci. *112*, 320–361. https://doi.org/10.1111/j.1749-6632.1964.tb26760.x.

36. Bromm, B., and Treede, R.D. (1987). Human cerebral potentials evoked by CO2 laser stimuli causing pain. Exp. Brain Res. *67*, 153–162. https://doi.org/10.1007/BF00269463.

37. Hu, L., Mouraux, A., Hu, Y., and Iannetti, G.D. (2010). A novel approach for enhancing the signal-to-noise ratio and detecting automatically event-related potentials (ERPs) in single trials. Neuroimage *50*, 99–111. https://doi.org/10.1016/j.neuroimage.2009.12.010.

38. Odom, J.V., Bach, M., Brigell, M., Holder, G.E., McCulloch, D.L., Mizota, A., and Tormene, A.P.; International Society for Clinical Electrophysiology of Vision (2016). ISCEV standard for clinical visual evoked potentials: (2016 update). Doc. Ophthalmol. *133*, 1–9. https://doi.org/10.1007/s10633-016-9553-y.

39. Cruccu, G., Aminoff, M.J., Curio, G., Guerit, J.M., Kakigi, R., Mauguiere, F., Rossini, P.M., Treede, R.-D., and Garcia-Larrea, L. (2008). Recommendations for the clinical use of somatosensory-evoked potentials. Clin. Neurophysiol. *119*, 1705–1719. https://doi.org/10.1016/j.clinph.2008.03.016.

40. Apkarian, A.V., Bushnell, M.C., Treede, R.D., and Zubieta, J.K. (2005). Human brain mechanisms of pain perception and regulation in health and disease. Eur. J. Pain *9*, 463. https://doi.org/10.1016/j.ejpain.2004.11.001.

41. Iannetti, G.D., and Mouraux, A. (2010). From the neuromatrix to the pain matrix (and back). Exp. Brain Res. *205*, 1–12.

42. Legrain, V., Iannetti, G.D., Plaghki, L., and Mouraux, A. (2011). The pain matrix reloaded: a salience detection system for the body. Prog. Neurobiol. *93*, 111–124.

43. Xu, A., Larsen, B., Baller, E.B., Scott, J.C., Sharma, V., Adebimpe, A., Basbaum, A.I., Dworkin, R.H., Edwards, R.R., Woolf, C.J., et al. (2020). Convergent neural representations of experimentally-induced acute pain in healthy volunteers: a large-scale fMRI meta-analysis. Neurosci. Biobehav. Rev. *112*, 300–323. https://doi.org/10.1016/j.neubiorev.2020.01.004.

44. Mouraux, A., and Plaghki, L. (2007). Cortical interactions and integration of nociceptive and non-nociceptive somatosensory inputs in humans. Neuroscience *150*, 72–81. https://doi.org/10.1016/j.neuroscience.2007.08.035.

45. Granovsky, Y., Granot, M., Nir, R.R., and Yarnitsky, D. (2008). Objective correlate of subjective pain perception by contact heat-evoked potentials. J. Pain *9*, 53–63. https://doi.org/10.1016/j.jpain.2007.08.010.

46. Carmon, A., Dotan, Y., and Sarne, Y. (1978). Correlation of subjective pain experience with cerebral evoked responses to noxious thermal stimulations. Exp. Brain Res. *33*, 445–453. https://doi.org/10.1007/BF00235566.

47. Bornhövd, K., Quante, M., Glauche, V., Bromm, B., Weiller, C., and Büchel, C. (2002). Painful stimuli evoke different stimulus–response functions in the amygdala, prefrontal, insula and somatosensory cortex: a single-trial fMRI study. Brain *125*, 1326–1336. https://doi.org/10.1093/brain/awf137.

48. Hoeppli, M.E., Nahman-Averbuch, H., Hinkle, W.A., Leon, E., Peugh, J., Lopez-Sola, M., King, C.D., Goldschneider, K.R., and Coghill, R.C. (2022). Dissociation between individual differences in self-reported pain intensity and underlying fMRI brain activation. Nat. Commun. *13*, 3569. https://doi.org/10.1038/s41467-022-31039-3.

49. Tiemann, L., Hohn, V.D., Ta Dinh, S., May, E.S., Nickel, M.M., Gross, J., and Ploner, M. (2018). Distinct patterns of brain activity mediate perceptual and motor and autonomic responses to noxious stimuli. Nat. Commun. *9*. https://doi.org/10.1038/s41467-018-06875-x.

50. Novembre, G., Pawar, V.M., Bufacchi, R.J., Kilintari, M., Srinivasan, M., Rothwell, J.C., Haggard, P., and Iannetti, G.D. (2018). Saliency detection as a reactive process: unexpected sensory events evoke corticomuscular coupling. J. Neurosci. *38*, 2385–2397.

51. Moayedi, M., Liang, M., Sim, A.L., Hu, L., Haggard, P., and Iannetti, G.D. (2015). Laser-evoked vertex potentials predict defensive motor actions. Cereb. Cortex *25*, 4789–4798.

52. Garcia-Larrea, L., Frot, M., and Valeriani, M. (2003). Brain generators of laser-evoked potentials: from dipoles to functional significance. Neurophysiol. Clin. Neurophysiol. *33*, 279–292. https://doi.org/10.1016/j.neucli.2003.10.008.

53. Valentini, E., Hu, L., Chakrabarti, B., Hu, Y., Aglioti, S.M., and Iannetti, G.D. (2012). The primary somatosensory cortex largely contributes to the early part of the cortical response elicited by nociceptive stimuli. Neuroimage *59*, 1571–1581. https://doi.org/10.1016/j.neuroimage.2011.08.069.

54. Iannetti, G.D., Hughes, N.P., Lee, M.C., and Mouraux, A. (2008). Determinants of laser-evoked EEG responses: pain perception or stimulus saliency? J. Neurophysiol. *100*, 815–828. https://doi.org/10.1152/jn.00097.2008.

55. Mouraux, A., Diukova, A., Lee, M.C., Wise, R.G., and Iannetti, G.D. (2011). A multisensory investigation of the functional significance of the "pain matrix". Neuroimage *54*, 2237–2249.

56. Ronga, I., Valentini, E., Mouraux, A., and Iannetti, G.D. (2012). Novelty is not enough: laser-evoked potentials are determined by stimulus saliency, not absolute novelty. J. Neurophysiol. *109*, 692–701. https://doi.org/10.1152/jn.00464.2012.

57. Su, Q., Qin, W., Yang, Q.Q., Yu, C.S., Qian, T.Y., Mouraux, A., Iannetti, G.D., and Liang, M. (2019). Brain regions preferentially responding to transient and iso-intense painful or tactile stimuli. Neuroimage *192*, 52–65. https://doi.org/10.1016/j.neuroimage.2019.01.039.

58. Wang, A.L., Mouraux, A., Liang, M., and Iannetti, G.D. (2010). Stimulus novelty, and not neural refractoriness, explains the repetition suppression of laser-evoked potentials. J. Neurophysiol. *104*, 2116–2124. https://doi.org/10.1152/jn.01088.2009.

59. Poldrack, R.A. (2006). Can cognitive processes be inferred from neuroimaging data? Trends Cogn. Sci. *10*, 59–63.

60. Lee, M.C., Mouraux, A., and Iannetti, G.D. (2009). Characterizing the cortical activity through which pain emerges from nociception. J. Neurosci. *29*, 7909–7916. https://doi.org/10.1523/JNEUROSCI.0014-09.2009.

61. Willis, W.D., and Westlund, K.N. (1997). Neuroanatomy of the pain system and of the pathways that modulate pain. J. Clin. Neurophysiol. *14*, 2–31.

62. Hecht, S. (1936). Intensity discrimination and its relation to the adaptation of the eye. J. Physiol. *86*, 15–21.

63. Carlyon, R.P., and Moore, B.C.J. (1984). Intensity discrimination: a severe departure from Weber's law. J. Acoust. Soc. Am. *76*, 1369–1376. https://doi.org/10.1121/1.391453.

64. Nelson, D.A., Schmitz, J.L., Donaldson, G.S., Viemeister, N.F., and Javel, E. (1996). Intensity discrimination as a function of stimulus level with electric stimulation. J. Acoust. Soc. Am. *100*, 2393–2414. https://doi.org/10.1121/1.417949.

65. Rollman, G.B., and Harris, G. (1987). The detectability, discriminability, and perceived magnitude of painful electrical shock. Percept. Psychophys. *42*, 257–268. https://doi.org/10.3758/BF03203077.

66. Sakitt, B. (1972). Counting every quantum. J. Physiol. *223*, 131–150. https://doi.org/10.1113/jphysiol.1972.sp009838.

67. Heywood, C.A., and Cowey, A. (1986). The nature of the visual discrimination impairment after neonatal or adult ablation of superior colliculi in rats. Exp. Brain Res. *61*, 403–412. https://doi.org/10.1007/BF00239529.

68. Johnson, K.O., Darian-Smith, I., LaMotte, C., Johnson, B., and Oldfield, S. (1979). Coding of incremental changes in skin temperature by a population of warm fibers in the monkey: correlation with intensity discrimination in man. J. Neurophysiol. *42*, 1332–1353. https://doi.org/10.1152/jn.1979.42.5.1332.

69. Vierck, C.J. (1977). Absolute and differential sensitivities to touch stimuli after spinal cord lesions in monkeys. Brain Res. *134*, 529–539. https://doi.org/10.1016/0006-8993(77)90827-7.

70. Flor, H., Denke, C., Schaefer, M., and Grüsser, S. (2001). Effect of sensory discrimination training on cortical reorganisation and phantom limb pain. Lancet *357*, 1763–1764. https://doi.org/10.1016/S0140-6736(00)04890-X.

71. Pleger, B., Tegenthoff, M., Ragert, P., Förster, A.F., Dinse, H.R., Schwenkreis, P., et al. (2005). Sensorimotor returning in complex regional pain syndrome parallels pain reduction. Ann. Neurol. *57*, 425–429. https://doi.org/10.1002/ana.20394.

72. Delorme, A., and Makeig, S. (2004). EEGLAB: an open source toolbox for analysis of single-trial EEG dynamics including independent component analysis. J. Neurosci. Methods *134*, 9–21.

73. Hu, L., Xiao, P., Zhang, Z.G., Mouraux, A., and Iannetti, G.D. (2014). Single-trial time–frequency analysis of electrocortical signals: baseline correction and beyond. Neuroimage *84*, 876–887.

74. Peng, W.W., Tang, Z.Y., Zhang, F.R., Li, H., Kong, Y.Z., Iannetti, G.D., and Hu, L. (2019). Neurobiological mechanisms of TENS-induced analgesia. Neuroimage *195*, 396–408. https://doi.org/10.1016/j.neuroimage.2019.03.077.

75. Macmillan, N.A., and Creelman, C.D. (2004). Detection Theory: A User's Guide (Psychology Press).

76. Kemperman, I., Russ, M.J., Clark, W.C., Kakuma, T., Zanine, E., and Harrison, K. (1997). Pain assessment in self-injurious patients with borderline personality disorder using signal detection theory. Psychiatry Res. *70*, 175–183. https://doi.org/10.1016/s0165-1781(97)00034-6.

77. Wright, D.B., Horry, R., and Skagerberg, E.M. (2009). Functions for traditional and multilevel approaches to signal detection theory. Behav. Res. Methods *41*, 257–267. https://doi.org/10.3758/BRM.41.2.257.

78. Benjamini, Y., and Hochberg, Y. (1995). Controlling the false discovery rate: a practical and powerful approach to multiple testing. J. R. Stat. Soc. Ser. B *57*, 289–300.

79. Keysers, C., Gazzola, V., and Wagenmakers, E.J. (2020). Using Bayes factor hypothesis testing in neuroscience to establish evidence of absence. Nat. Neurosci. *23*, 788–799. https://doi.org/10.1038/s41593-020-0660-4.

80. Kass, R.E., and Raftery, A.E. (1995). Bayes factors. J. Am. Stat. Assoc. *90*, 773–795. https://doi.org/10.1080/01621459.1995.10476572.

81. Buitinck, L., Louppe, G., Blondel, M., Pedregosa, F., Mueller, A., Grisel, O., Niculae, V., Prettenhofer, P., Gramfort, A., Grobler, J., et al. (2013). API design for machine learning software: experiences from the scikit-learn project. https://doi.org/10.48550/arXiv.1309.0238.

82. Ashburner, J., and Friston, K.J. (2005). Unified segmentation. Neuroimage *26*, 839–851. https://doi.org/10.1016/j.neuroimage.2005.02.018.

83. Coghill, R.C., Talbot, J.D., Evans, A.C., Meyer, E., Gjedde, A., Bushnell, M.C., and Duncan, G.H. (1994). Distributed processing of pain and vibration by the human brain. J. Neurosci. *14*, 4095–4108. https://doi.org/10.1523/JNEUROSCI.14-07-04095.1994.

84. Jones, A.K.P., Brown, W.D., Friston, K.J., Qi, L.Y., and Frackowiak, R.S.J. (1991). Cortical and subcortical localization of response to pain in man using positron emission tomography. Proc. R. Soc. Lond. B Biol. Sci. *244*, 39–44. https://doi.org/10.1098/rspb.1991.0048.

85. Talbot, J.D., Marrett, S., Evans, A.C., Meyer, E., Bushnell, M.C., and Duncan, G.H. (1991). Multiple representations of pain in human cerebral cortex. Science *251*, 1355–1358. https://doi.org/10.1126/science.2003220.

86. Holm, S. (1979). A simple sequentially rejective multiple test procedure. Scand. J. Stat. *6*, 65–70.

87. Desikan, R.S., Ségonne, F., Fischl, B., Quinn, B.T., Dickerson, B.C., Blacker, D., Buckner, R.L., Dale, A.M., Maguire, R.P., Hyman, B.T., et al. (2006). An automated labeling system for subdividing the human cerebral cortex on MRI scans into gyral based regions of interest. Neuroimage *31*, 968–980. https://doi.org/10.1016/j.neuroimage.2006.01.021.

88. Geuter, S., Boll, S., Eippert, F., and Büchel, C. (2017). Functional dissociation of stimulus intensity encoding and predictive coding of pain in the insula. Elife *6*. https://doi.org/10.7554/eLife.24770.

89. Yarkoni, T., Poldrack, R.A., Nichols, T.E., Van Essen, D.C., and Wager, T.D. (2011). Large-scale automated synthesis of human functional neuroimaging data. Nat. Methods *8*, 665–670.

STAR★METHODS

KEY RESOURCES TABLE

REAGENT or RESOURCE	SOURCE	IDENTIFIER
Deposited data		
Datasets	OSF	https://doi.org/10.17605/OSF.IO/S4UGW
Unthresholded statistical maps	OSF	https://doi.org/10.17605/OSF.IO/S4UGW
Software and algorithms		
MATLAB (R2016a)	MathWorks	https://www.mathworks.com/
EEGLAB (2019_1)	Delorme and Makeig, 2004	https://sccn.ucsd.edu/eeglab/index.php
SPM 12	Wellcome Trust Center for Neuroimaging	https://www.fil.ion.ucl.ac.uk/spm/software/spm12/
jamovi (1.8.1.0)	The jamovi project	https://www.jamovi.org/
R/Rstudio (4.1.2/554)	Rstudio	https://www.r-project.org/, https://www.rstudio.com
Python (3.9)	Python Software Foundation	https://www.python.org/
Data analysis scripts	This paper	https://doi.org/10.17605/OSF.IO/S4UGW

RESOURCE AVAILABILITY

Lead contact

Further information and requests for resources should be directed to and will be fulfilled by the lead contact, Li Hu (huli@psych.ac.cn).

Materials availability

This study did not generate new unique reagents.

Data and code availability

- The data used for all figures and tables of the paper has been deposited on the Open Science Framework (https://doi.org/10.17605/OSF.IO/S4UGW).
- All original analysis code (i.e., code for computing discriminability indices, matching ratings between pairs of modalities, and predicting pain discriminability with LEP and fMRI responses using machine learning) has been deposited on the Open Science Framework (https://doi.org/10.17605/OSF.IO/S4UGW).
- Any additional information required to reanalyze the data reported in this paper is available from the Lead contact upon reasonable request.

EXPERIMENTAL MODEL AND SUBJECT DETAILS

Five large datasets, which have not been published before in their entirety, were collected for this paper. Datasets 1, 2, and 3 were for EEG studies and included 366 healthy participants in total: (i) Dataset 1, 114 participants (40 males) aged 20.7 ± 2.3 years (mean ± SD); (ii) Dataset 2, 111 participants (54 males) aged 20.9 ± 2.3 years; (iii) Dataset 3, 141 participants (54 males) aged 21.8 ± 4.7 years. Datasets 4 and 5 were for fMRI studies and collected from 399 healthy participants: (i) Dataset 4, 212 participants (One participant did not provide the demographic information. For the rest 211 participants, 76 males, aged 21.5 ± 4.2 years); (ii) Dataset 5, 187 participants (One participant did not provide the demographic information. For the rest 186 participants, 84 males, aged 21.0 ± 3.3 years). All participants were pain-free and had no history of chronic pain, neurological or psychiatric illness. They all gave written informed consent and were paid for their participation. The procedures were approved by the local ethics committee at the Institute of Psychology, Chinese Academy of Sciences.

METHOD DETAILS

EEG studies

We collected three large EEG datasets, in which signals were recorded from healthy participants with different pain sensitivity using different EEG systems (Figure 1A). Dataset 1 included participants with high pain sensitivity and was recorded using the BP EEG system. Datasets 2 and 3 included participants with low pain sensitivity and were recorded using the BP EEG system and the Biosemi EEG system, respectively.

Sensory stimulation

In each experiment, participants received transient stimuli belonging to four different sensory modalities: nociceptive laser, non-nociceptive tactile, auditory, and visual. For each sensory modality, two stimulus intensities (i.e., high and low) were delivered (Figure 1C). In other words, each participant underwent eight experimental conditions (4 modalities×2 intensities).

Painful stimuli were transient radiant heat pulses (wavelength: 1.34μm; pulse duration: 4ms) generated by an infrared neodymium yttrium aluminum perovskite (Nd: YAP) laser (Electronical Engineering, Italy). The laser beam was transmitted by an optic fiber, and its diameter was set at approximately 7mm. Laser pulses were delivered to a pre-defined square (5 × 5cm^2) on the left hand dorsum. After each stimulus, the laser beam was displaced by approximately 1cm in a random direction to avoid nociceptor fatigue or sensitization. Two stimulus energies (3.0 and 3.5J) were used in Dataset 1, which included participants with high pain sensitivity. Two higher stimulus energies (3.5 and 4.0J) were used in Datasets 2 and 3, which included participants with low pain sensitivity (see below for the procedure used to assign participants to the two datasets). Non-nociceptive tactile stimuli were constant current square-wave electrical pulses (duration: 1ms; model DS7A, Digitimer, UK) delivered through a pair of skin electrodes (1cm interelectrode distance) placed on the left wrist, over the superficial radial nerve. The same two stimulus intensities (2.0 and 4.0mA) were used in all three datasets. Auditory stimuli were brief pure tones (frequency: 800Hz; duration: 50ms; 5ms rise and fall time) delivered through a headphone. The same two stimulus intensities (76dB SPL and 88dB SPL) were used for all participants. Visual stimuli were brief flashes of a gray round disk in a black background (duration: 100ms) on a computer screen. The stimulus intensities were adjusted using the greyscale of the round disk, which corresponded to RGB values of (100, 100, 100) and (200, 200, 200), respectively.

After each stimulus, participants were asked to verbally rate the perceived intensity using an NRS ranging from 0 ("no sensation") to 10 ("the strongest sensation imaginable [in each stimulus modality]"). Stimulus intensities of tactile, auditory, and visual stimuli were determined based on a pilot behavioral experiment to ensure that the perceived ratings of low and high intensity stimuli were approximately 4 and 7 out of 10, respectively. However, since nociceptive laser stimuli of 4.0J were unbearable for some participants, we divided all participants into two groups, i.e., high and low pain sensitivity participants. High-pain-sensitivity participants were those who rated 4.0J laser stimuli >8. All remaining participants, who rated the 4.0J stimuli $\leq$8, were assigned to the low-pain-sensitivity datasets.

Rating and AUC matching procedures

Since the perceptual ratings may not be comparable between different sensory modalities, any difference in the relationship between EEG responses and discriminability indices across modalities could be due to the difference in perceptual ratings. To control for this possible confounding factor, we adopted a rating matching procedure to equalize intensity ratings between pairs of sensory modalities (i.e., pain vs. touch, pain vs. audition, and pain vs. vision) in the BP Dataset (including all data from Datasets 1 and 2) and the BioSemi Dataset (i.e., Dataset 3), respectively.

The matching procedure was adapted from a previous study.[24] Take the matching between pain and touch as an example – suppose Participant X rated the high- and low-intensity laser stimuli as 6 and 4 on average, respectively. We search for all participants whose mean ratings for high-intensity tactile stimuli are within the range of 5.5–6.5 AND mean ratings for low-intensity tactile stimuli are within the range of 3.5–4.5. In other words, the absolute average matching error should be $\leq$ 0.5 for both high- and low-intensity stimuli. Assume that M participants would be qualified according to the absolute matching error criterion. Among them, N participants have the smallest absolute matching error. If N = 1, Participant X is finally paired with this single participant; if N > 1, Participant X is finally paired with a random member (say, Y) in the N participants, given that Participant Y has not been paired with any other participant.

We also used an AUC matching procedure to account for the apparent ceiling effect of the discriminability measure (i.e., AUC; see Discriminability measures below for more information; Figure 4). The AUC matching procedure was almost identical to the rating matching procedure, except that the absolute average matching error was 0.1 instead of 0.5 since AUC can only take values between 0 and 1. To maximize statistical power, we pooled all participants in the three EEG datasets (N = 366) in the AUC matching procedure.

Experimental procedures

Experimental procedures were identical in the three datasets (Figure 1C). Participants were seated in a comfortable chair in a dim, silent, and temperature-controlled room. The experiment consisted of three blocks, and, in each block, 40 sensory stimuli (5 stimuli for each modality and intensity) were delivered while the EEG signals were recorded. After each block, participants were allowed to take a brief break. The order of stimulus modality and intensity was pseudo-randomized in each block. Each trial began with a fixation cross, which, after 3000ms, was followed by a transient sensory stimulus. 3000ms after the stimulus, participants were required to verbally rate the perceived intensity using a 0–10 NRS within 5000ms. Between 1000ms and 3000ms after the rating period, a new trial started. The inter-stimulus interval thus ranged between 12000ms and 14000ms.

EEG recording

EEG data were acquired via 64 AgCl electrodes positioned according to the International 10–20 System, using the nose as reference (band-pass filter: 0.01Hz–100Hz; sampling rate: 1000Hz; Brain Products EEG system, Germany for Datasets 1 and 2; BioSemi EEG system, Netherlands for Dataset 3). Electrode impedance was kept lower than 10kΩ. Electrooculographic signals were simultaneously recorded using two surface electrodes, one placed ~10mm below the left eye and the other placed ~10mm from the outer canthus of the left eye.

fMRI studies

To assess whether EEG findings could be generalized in fMRI data, we collected two large fMRI datasets (i.e., Datasets 4 and 5), in which signals were collected from healthy participants with high or low pain sensitivity, respectively (Figure 1B).

Sensory stimulation

Sensory stimuli used in the fMRI studies were identical to those in the EEG studies, except that visual stimuli were presented on a screen via an MRI-compatible projector. Since participants in Dataset 4 were more pain-sensitive, they received painful laser stimuli of 3.0J (low intensity) and 3.5J (high intensity). Participants in Dataset 5 were less pain-sensitive and received laser stimuli of 3.5J (low intensity) and 4.0J (high intensity).

Experimental procedures

Experimental procedures in Datasets 4 and 5 were identical, and both were similar to the EEG studies (Figure 1D). The experiment comprised two blocks, and in each block, 40 sensory stimuli (5 stimuli for each modality and intensity) were delivered in the MRI scanner. The order of stimulus modality and intensity within each block was pseudo-randomized. Each trial began with a 6000ms fixation cross, which was followed by a transient sensory stimulus. 10000ms after the stimulus, participants were asked to move a slide to rate the perceived intensity using the 0–10 NRS shown on the screen within 5000ms. A new trial started after an interval of 1000ms or 2000ms. The inter-stimulus interval thus ranged between 22000ms and 23000ms.

MRI acquisition

Whole brain MRI data were collected using a 3.0 Telsa MRI system (Discovery MR 750; General Electric Healthcare, Milwaukee, WI, USA) at the Research Center of Brain Cognitive Neuroscience at Liaoning Normal University, China. Functional images were obtained using a T2*-weighted Gradient Echo sequence (repetition time = 2000ms, echo time = 29ms, interleaved slices = 43, slice thickness = 3.0mm, inter-slice gap = 0mm, acquisition matrix = 64 × 64, flip angle = 90°, field of view = 192 × 192mm^2, in-plane resolution = 3 × 3mm^2). A high-resolution, 3D T1-weighted image was also acquired using a spoiled gradient-recalled echo (SPGR) sequences (field of view = 256 × 256mm^2, in-plane resolution = 1 × 1mm^2) before functional imaging acquisition.

QUANTIFICATION AND STATISTICAL ANALYSIS

EEG studies

EEG data processing

EEG data were processed in MATLAB (R2016a; MathWorks, USA) using the EEGLAB toolbox.[72] Continuous EEG data were band-pass filtered between 1 and 30Hz for time-domain analyses, and between 1 and 100Hz for time-frequency analyses. Subsequently, EEG data were segmented into epochs extending from 1000ms before to 2000ms after stimulus onset. Each epoch was baseline corrected using the prestimulus interval. Bad electrodes (i.e., Fp1, Fp2, F1, and F2 in some participants) were replaced using spherical interpolation. Trials contaminated by eye blinks and movements were corrected using an independent component analysis algorithm (“runica”) implemented in the EEGLAB toolbox.[72]

For each participant, single-trial EEG waveforms of each of the 8 conditions (4 modalities×2 intensities) were averaged. Baseline-to-peak amplitudes of the main negative and positive ERP waves (e.g., N2 and P2 waves) were measured in each participant for each condition. N2 and P2 waves were defined as the most negative and positive deflections at Cz between 100ms and 600ms after stimulus onset. To extract the component that is particularly tight to the afferent spinothalamic nociceptive input, we also measured the peak amplitude of the N1 wave in LEPs. N1 was defined as the most negative deflection preceding the N2 wave in LEPs, and measured at the central electrode contralateral to the stimulated side (i.e., C4), referenced to Fz.[37] To examine early components in other modalities, we also re-referenced EEG signals evoked by non-painful stimuli to Fz, following recommendations by previous studies.[38,39] Scalp topographies at N1, N2, and P2 peak latencies were computed by spline interpolation. Differential ERP amplitudes were calculated by subtracting the amplitudes evoked by low-intensity stimuli from those evoked by high-intensity stimuli for each sensory modality (i.e., high–low). Mean ERP amplitudes of laser-evoked N1, N2, and P2 waves were also obtained by calculating the averaged amplitudes evoked by low and high intensity stimuli (i.e., [high+low]/2) to assess whether LEPs could reflect pain sensitivity across individuals.

To identify event-related spectral perturbations associated with sensory discriminability, we also performed a time-frequency analysis on single-trial EEG responses. Specifically, a time-frequency distribution (TFD) of the EEG responses was obtained using a short-time Fourier transform (STFT) with a fixed 200-ms Hanning window. For each EEG trial, the STFT yielded a complex time-frequency estimate F(t, f) at each point (t, f) of the time-frequency plane, extending from −500ms to 1000ms (in steps of 2ms) in the time domain and from 1Hz to 100Hz (in steps of 2Hz) in the frequency domain. The resulting spectrogram, $P(t, f) = |F(t, f)|^2$, represents the signal power as a joint function of time and frequency at each time-frequency point. The spectrogram was then baseline-corrected (baseline interval: −400ms ∼ -100 ms) at each frequency using the subtraction method.[73] According to previous studies,[22,74] the magnitudes of two time-frequency features (i.e., gamma-band event-related synchronization [γ-ERS] and alpha-band event-related desynchronization [α-ERD]) were extracted for each participant, by computing the top 20% of all time-frequency points within their respective time-frequency regions-of-interest (TF-ROIs): γ-ERS (100ms–300ms, 60Hz–90 Hz at Cz), α-ERD (500ms–900 ms, 7Hz–13 Hz at POz). Differential magnitudes of event-related spectral perturbations were calculated by subtracting the magnitudes evoked by low-intensity stimuli from those evoked by high-intensity stimuli for each sensory modality (i.e., high–low).

Discriminability measures

For each sensory modality, discriminability was quantified using two SDT-derived measures (i.e., AUC, d′). Like the difference threshold in traditional psychophysics, these measures quantify the ability to discriminate between different stimuli. While the difference threshold holds constant sensation (i.e., just noticeable difference) and uses the difference in physical intensities between the

two stimuli to quantify discriminability, these measures fix the physical intensities and quantify discriminability using the difference of sensation between stimuli. However, unlike the difference threshold, SDT is a powerful tool for separating discriminability from response criteria (e.g., the tendency to report one stimulus as more painful) and thus minimizing the influence of response criteria on discriminability.[4,75] Practically speaking, measuring the difference threshold could be more time-consuming and may also be unsuitable using a laser device, as the laser energy can't be set arbitrarily. For the Nd: YAP laser (Stimul 1340, Electronical Engineering, Italy) that was equipped in our lab, the smallest energy difference between two stimuli is 0.25J (e.g., 3.00 vs 3.25J), which may be too large to precisely measure the difference threshold for some participants. These considerations prompted us to quantify discriminability using the SDT-derived measures.

AUC is an oft-used nonparametric measure of discriminability.[8,28,76] Importantly, we did not use the typical SDT design in which participants are required to identify one of two alternative stimuli (e.g., the stronger stimuli of two intensities).[27] Rather, we used a rating design in the framework of SDT,[27] which is particularly suitable for computing AUC values[29] and has been used extensively in many classic pain behavioral studies.[1–3,28] In the rating design,[1–3,28] participants report how painful a pain stimulus is on a numerical rating scale. This is equivalent to treating every numerical rating (0–10) on the scale as an implicit criterion. In order to compute AUC values, for a given criterion (e.g., 5), ratings greater than or equal to this criterion (i.e., 5–10) in the high-intensity condition are hit responses, while ratings greater than or equal to this criterion in the low-intensity condition are false alarms (Figure 1E). The hit rate is obtained by dividing the number of hit responses by the number of total trials in the high-intensity condition. The false alarm rate is the proportion of false alarms in the low-intensity condition. A hit rate-false alarm rate pair defines a point on the ROC curve. Since there are 11 integral ratings on the NRS, there will be 11 points on the ROC curve, and the AUC value is defined as the area under the ROC curve.

To demonstrate that our findings were not influenced by the choice of discriminability measure, we also quantified the discriminability using d′, a more widely-used parametric measure in SDT. Briefly, d′ = Z(hit rate)–Z(false alarm rate), where Z( ) is the inverse cumulative distribution function of the standard normal distribution.[27] To define hit responses and false alarms, we first pooled perceived ratings in high- and low-intensity conditions for each sensory modality and each participant. Then, we defined a series of cutoffs based on rating percentiles (from 5% to 95%, in steps of 5%, 19 cutoffs in total).[26] For a given cutoff percentile, ratings in the high-intensity condition were treated as hit responses if higher than the defined cutoff percentile, and ratings in the low-intensity condition were regarded as false alarms if higher than the cutoff percentile. As such, 19 d′ values could be computed, and the mean of these 19 d′ values was calculated as the measure of sensory discriminability.[26] Note that we added a flattening constant of 0.5 to the formula computing hit rates and false alarm rates since Z values would be infinite if hit rates or false alarm rates were 100% or 0%.[77] As a result, hit rates were defined as (hit response counts+0.5)/(total number of trials in the high-intensity condition+0.5*2), and false alarm rates as (false alarm counts+0.5)/(total number of trials in the low-intensity condition+0.5*2).

The main advantage of SDT-based measures (AUC and d′) is that discriminability can be separated from individual response, and thus the potential influence of individuals' response criteria on discriminability can be controlled and minimized.[4,75] However, these measures (especially AUC) may suffer from the ceiling effect if there is little overlapping of intensity ratings between stimuli. Unlike AUC and d', the rating difference (high–low), a very crude measure of discriminability, is unlikely to be saturated at some extreme values and thus does not suffer from the ceiling effect. We thus also adopted the rating difference as the third discriminability measure to assess the robustness of our findings based on SDT-based measures.

Computing these three measures unbiasedly requires that the number of intensity ratings in all four modalities is identical. Luckily, only one participant in Dataset 2 failed to provide a rating in one trial in the high-intensity tactile condition, and two participants in Dataset 3 did not report ratings in one trial (in the low-intensity auditory and low-intensity laser conditions, respectively). We imputed these three missing values from the mean rating in the respective condition for the corresponding participant.

Machine learning

We trained least absolute shrinkage and selection operator (LASSO) regression models[33] to predict pain AUC values using preprocessed LEP signals in Dataset 1. The LASSO is a regularization method that shrinks the linear regression coefficient estimates toward zero. Mathematically, LASSO regression minimizes the following loss function:

$$Loss = \sum_{i=1}^{n}\left(y_i - \beta_0 - \sum_{j=1}^{p}\beta_j x_{ij}\right)^2 + \lambda\sum_{j=1}^{p}|\beta_j|$$

where y_i is the predicted variable (or feature) of participant i, β_0 and β_j are the linear regression coefficient estimates, x_{ij} is the j-th predictor for participant i, and λ is the tuning parameter.

We used differences of peak amplitudes and latencies of N2 and P2 waves between high- and low-intensity conditions in Dataset 1 as predictors. As such, 236 predictors (2 peaks [N2 and P2] × 2 features [amplitude and latency] × 59 electrodes) were thus extracted for each participant. 10-fold cross-validation was used to evaluate model performance. That is, 114 participants in Dataset 1 were randomly divided into 10 groups with an almost equal number of participants, and one group was used as the test set, the other nine as the training set. The same procedure was repeated 10 times to ensure that every group was in the test set once. In each repeat, we first selected in the training set 20% of features that had the largest absolute values of univariate Pearson's correlation coefficients with pain AUC values, and then normalized all LEP predictors using z-scores to control the scale differences between different features. These z-scored features were then used to train the LASSO regression. Note that the feature selection (i.e., top 20% of

features) and normalization parameters were derived from the training set and applied to the test set to avoid data leakage. To determine the optimal tuning parameter λ, we selected 100 λ values log-uniformly distributed in the $[10^{-5}, 10^{-0.5}]$ interval and tuned λ using nested 10-fold cross-validation. The predictive performance of the final model was assessed using Pearson's correlation coefficient between the predicted and real pain AUC values. To examine the generalizability of the model, we applied the model to predicting pain AUC values in Dataset 2. The selectivity of the model was assessed by applying the model to predicting tactile, auditory, and visual AUC values in Dataset 1&2.

Statistical analysis

To assess whether participants were able to discriminate between two stimuli of different intensities, perceptual ratings and neural responses (e.g., N1, N2, and P2 amplitudes) evoked by high-intensity stimuli were compared with those evoked by low-intensity stimuli using paired-sample t-tests. Moreover, AUC values were compared with the chance level of 0.5 using one-sample t-tests. To identify EEG indicators of sensory discriminability, we correlated differential EEG responses (high–low) with AUC values using both parametric (Pearson's r) and nonparametric (Kendall's tau-b) correlation analyses. Correlation results were confirmed using point-by-point parametric correlation analyses with false discovery rate (FDR) correction.[78]

Bayesian correlation analysis was also conducted to provide direct evidence for or against the null hypothesis. Bayesian correlation analysis was conducted under the uninformative prior distribution of Beta(1, 1) to explicitly provide evidence for or against the null hypothesis of no correlation.[79] The Bayes factor (BF), a key index in Bayesian statistics, quantifies the relative likelihood of collecting the data given the alternative hypothesis over the null hypothesis.[79] Different BF values were interpreted in the way recommended by Kass & Raftery[80]: (i) 1–3.2: barely worth mentioning evidence for the alternative hypothesis; (ii) 3.2–10: substantial evidence; (iii) 10–100: strong evidence; (iv) > 100: decisive evidence. The reciprocal of BF values less than 1 can be interpreted as evidence for the null hypothesis. For example, a BF of 0.2 (i.e., 1/5) indicates substantial evidence for the null hypothesis.

To determine whether the rating matching procedure was successful, we performed a two-way repeated-measures ANOVA ("modality": pain and touch, for instance; "intensity": low-intensity and high-intensity). Intensity rating differences between pairs of sensory modalities (e.g., pain vs. touch) were considered equalized if there was not a significant interaction effect. If the rating matching procedure was successful, we then performed the correlation analyses to demonstrate the pain-selectivity of the correlation between EEG responses and AUC values using the rating-matched datasets. Additionally, we directly assessed the possible difference of correlation coefficients between different sensory modalities using the *r.test* function in the R package *psych* (ver 2.1.6).

Point-by-point correlation analyses were conducted in MATLAB (R2016a; MathWorks, USA). All other statistical analyses were conducted in the open-source statistical software *jamovi* (ver. 1.8.1.0) (https://www.jamovi.org/). Bayesian analysis was performed based on the *JSQ-BAYESIAN METHODS* module (ver. 1.0.2) in *jamovi*. Machine learning modeling was conducted in Python (ver. 3.9; https://www.python.org/) using the sklearn library (ver. 1.1.2; https://scikit-learn.org/stable/).[81]

fMRI studies

Image preprocessing

fMRI data were preprocessed and analyzed using Statistical Parametric Mapping 12 (SPM12) (Wellcome Trust Center for Neuroimaging, London). The first three volumes in each run were discarded to allow for signal stabilization. Images were slice-time corrected using the second slice and realigned to the mean slice. The resulting images were normalized to the Montreal Neurological Institute (MNI) space (resampling voxel size = $3 \times 3 \times 3 mm^3$)[82] and then smoothed with a 6-mm full-width at half maximum (FWHM) Gaussian kernel.

fMRI analysis

First-level analyses were conducted using the general linear model. Regressors included eight conditions (4 modalities×2 intensities) convolved with the canonical hemodynamic response function and six head motion estimates. Moreover, we high-pass filtered images with a cutoff period of 128s and accounted for temporal autocorrelations using the first-order autoregressive model (AR(1)). Second-level analyses were performed to determine brain regions responding to stimuli of different intensities and brain regions associated with sensory discriminability. To these ends, four contrast images for four sensory modalities were first constructed for each participant: (1) pain: high intensity (high)–low intensity (low); (2) touch: high–low; (3) audition: high–low; (4) vision: high–low. Contrast images were then submitted to one-sample t-tests to assess the effect of stimulus intensity for each sensory modality. To identify brain regions responsible for sensory discriminability, contrast images entered linear regression models with AUC values as the predictor for each sensory modality. In whole-brain analyses, the significance threshold was set at $p = 0.001$ at the voxel level and $p_{FWE} = 0.05$ at the cluster level.

As in the EEG studies, the discriminability was quantified using three indices (i.e., AUC, d′, and rating differences) for each sensory modality. Additionally, the same rating matching procedure was performed to rule out the possible confounding factor due to the difference of perceptual ratings between modalities. To ensure that participants were able to discriminate between two stimuli of different intensities, perceptual ratings evoked by high-intensity stimuli were compared with those evoked by low-intensity stimuli using paired-sample t-tests. AUC values were compared with the chance level of 0.5 using one-sample t-tests. To assess the replicability of our findings, we used Dataset 4 to explore neural indicators of pain discriminability and used Dataset 5 to replicate the results obtained in Dataset 4. We first defined a series of ROIs, which were obtained by calculating the conjunction of brain regions with significant correlation with pain discriminability in Dataset 4 AND brain regions widely-accepted for pain processing (i.e., bilateral thalamus, S1, S2, insula, and ACC).[40,43,83–85] Average BOLD responses in these ROIs were then extracted and correlated with pain

AUC values in Dataset 5 using the same correlation analyses specified in the EEG studies. To account for the problem of multiple comparisons in the ROI-based correlation analysis, we corrected correlation results using the Holm correction method.[86] The anatomical locations of pain-related regions were defined using the Harvard-Oxford Atlas[87] distributed with FSL. The probability maps were thresholded at 50%.[88]

Machine learning

We also trained a LASSO regression model[33] to predict pain AUC values using laser-evoked fMRI signals in Dataset 4. The model was developed in a way similar to the LASSO regression model in the EEG studies. To account for the variation of fMRI signals, we used unthresholded first-level t maps for the contrast "high pain–low pain" as predictors. We first selected a set of brain areas that are related to the term "pain" using the association test (FDR-corrected $p < 0.01$) in the Neurosynth meta-analysis database[89] (https://neurosynth.org/) and extracted brain signals in this Neurosynth "pain" mask. We then further selected 20% of voxels that showed the largest absolute values of correlation coefficients with pain AUC values. Signals in these voxels were standardized across participants and submitted to principal component analysis to reduce the feature dimensions. A small number of principal components were retained so that they could explain 80% of variance of signals in the top 20% of voxels. These components were used as features in the LASSO regression model. 10-fold cross-validation was also used to evaluate model performance. The predictive performance of the final model was assessed using Pearson's correlation coefficient between the predicted and real AUC values. To examine the generalizability of the model, we applied the model to predicting pain AUC values in Dataset 5. The selectivity of the model was assessed by applying it to predicting tactile, auditory, and visual AUC values in Dataset 4&5.